© 2019. Published by The Company of Biologists Ltd | Journal of Cell Science (2019) 132, jcs224931. doi:10.1242/jcs.224931

RESEARCH ARTICLE

Phosphorylation at distinct subcellular locations underlies specificity in mTORC2-mediated activation of SGK1 and Akt

Catherine E. Gleason[1,*], Juan A. Oses-Prieto[2], Kathy H. Li[2], Bidisha Saha[1], Gavin Situ[1], Alma L. Burlingame[2] and David Pearce[1]

ABSTRACT

mTORC2 lies at the intersection of signaling pathways that control metabolism and ion transport through phosphorylation of the AGC-family kinases, the Akt and SGK1 proteins. How mTORC2 targets these functionally distinct downstream effectors in a context-specific manner is not known. Here, we show that the salt- and blood pressure-regulatory hormone, angiotensin II (AngII) stimulates selective mTORC2-dependent phosphorylation of SGK1 (S422) but not Akt (S473 and equivalent sites). Conventional PKC (cPKC), a critical mediator of the angiotensin type I receptor (AT_1R, also known as AGTR1) signaling, regulates the subcellular localization of SIN1 (also known as MAPKAP1) and SGK1. Inhibition of cPKC catalytic activity disturbs SIN1 and SGK1 subcellular localization, re-localizing them from the nucleus and a perinuclear compartment to the plasma membrane in advance of hormonal stimulation. Surprisingly, pre-targeting of SIN1 and SGK1 to the plasma membrane prevents SGK1 S422 but not Akt S473 phosphorylation. Additionally, we identify three sites on SIN1 (S128, S315 and S356) that are phosphorylated in response to cPKC activation. Collectively, these data demonstrate that SGK1 activation occurs at a distinct subcellular compartment from that of Akt and suggests a mechanism for the selective activation of these functionally distinct mTORC2 targets through subcellular partitioning of mTORC2 activity.

KEY WORDS: mTORC2, SIN1, Akt, SGK, PKC, Angiotensin

INTRODUCTION

The mechanistic target of rapamycin (mTOR) is a key regulatory node in the signaling pathways that control numerous essential cellular and physiological functions including proliferation, growth, metabolism and ion balance. mTOR is the catalytic core of two functionally distinct multi-protein complexes, mTORC1 and mTORC2. Each complex interacts with a distinct set of targets enabling mTOR to respond uniquely to growth factors, nutrient availability and other stimuli. mTORC1 consists of mLST8, DEPTOR, PRAS40 (also known as AKT1S1) and RAPTOR (also known as RPTOR). mTORC2, also contains mLST8 and DEPTOR, but is defined by the presence of RICTOR, SIN1 (also known as MAPKAP1) and PROTOR (also known as PRR5) (Kennedy and Lamming, 2016). Only mTORC1 is acutely inhibited by the macrolide rapamycin owing to the presence of RAPTOR and absence of RICTOR. Consequently, mTORC1 signaling and physiological function are relatively well defined. Much less is known about mTORC2 signaling and function (Gaubitz et al., 2016).

The best-characterized mTORC2 substrates belong to the AGC family of serine/threonine kinases, which include Akt proteins (hereafter referred to generically as Akt unless a specific isoform is meant), serum/glucocorticoid-induced kinases (SGKs) and protein kinase C (PKC). mTORC2 directly phosphorylates two conserved motifs within the C-terminal tails of these kinases, termed the turn motif and hydrophobic motif (HM). In addition, they also require phosphorylation at a site within their activation loop (T-loop) in the kinase catalytic domain mediated by the 3-phosphoinositide-dependent protein kinase 1 (PDK1, also known as PDPK1). Phosphorylation of the turn motif site is generally thought to occur constitutively, during or soon after translation, and functions to increase protein stability and stabilize the active conformation of the kinase (Alessi et al., 2009). In contrast, HM phosphorylation is induced in response to PI3K activation. Phosphorylation at both the T-loop and HM sites is required for maximal kinase activity (Pearce et al., 2010).

Within the AGC family, SGK and Akt share the greatest degree of homology, as they possess a similar domain structure and ∼55% sequence identity through their catalytic domain (Park et al., 1999). As a result, Akt and SGK recognize a similar substrate consensus motif (R-x-R-x-x-S/T) and phosphorylate an overlapping, but not identical, set of proteins (Brunet et al., 2001; Collins et al., 2003; Pearce et al., 2010). Despite their considerable similarities, Akt and SGK family members exhibit distinct physiological functions *in vivo*. Akt2 plays a major role in regulation of metabolism (Toker and Marmiroli, 2014), whereas SGK1 is primarily implicated in the control of ion transport (Lang et al., 2006). Accordingly, they are activated under distinct physiological circumstances, and disruption of their function results in distinct pathophysiological consequences. For example, Akt2 dysregulation is implicated in the development of insulin resistance and diabetes (Toker and Marmiroli, 2014), while impaired SGK1 function contributes to defects in blood pressure control and electrolyte balance (Lang et al., 2006). How these related kinases respond to distinct physiological cues, and achieve functional specificity in their signaling outputs is not clear. One mechanism for controlling selective activation of SGK1 and Akt could occur through distinct regulation of their catalytic activities by mTORC2. How mTORC2 selectively regulates substrate activation is not currently known. This issue has important clinical implications in that hypertension is frequently a major complication associated with obesity and diabetes and an obligate parameter for the diagnosis of metabolic syndrome (Carey, 2011). The coincidence of these disease states likely reflects crosstalk in the signaling pathways that regulate Akt and SGK proteins, and emphasizes the need for greater understanding of the regulatory mechanisms that control mTORC2 activity and confer mTORC2 substrate selectivity.

[1]Department of Medicine, Division of Nephrology, UCSF, San Francisco, CA 94143, USA. [2]Departments of Chemistry and Pharmaceutical Chemistry, UCSF, San Francisco, CA 94143, USA.

*Author for correspondence (catie@circlepharma.com)

C.E.G., 0000-0002-0063-0729

Received 7 September 2018; Accepted 21 February 2019

Journal of Cell Science (2019) 132, jcs224931. doi:10.1242/jcs.224931

Recently, the mTORC2 subunit SIN1 has been implicated as a critical signaling integrator for mTORC2 activity. SIN1, along with RICTOR, is required for mTORC2 complex assembly (Gaubitz et al., 2016). In addition, SIN1 recruits several mTORC2 substrates to the complex through direct interaction (Cameron et al., 2011; Lu et al., 2011). We previously showed that mutation of a single amino acid (Q68) in SIN1 disrupts the interaction of SIN1 with SGK1 but not with Akt or PKC (Lu et al., 2011). This same mutation also disrupts mTORC2-dependent activation of SGK1, but not of Akt or PKC, demonstrating that mTORC2 can be induced to selectively activate one of its substrates, but not others, through mutation of one of its defining subunits, SIN1. More recently, several groups have demonstrated that growth factor signaling can influence mTORC2 activity through phosphorylation of different subunits. Growth factor-induced phosphorylation of RICTOR at T1135 by p70S6K (also known as RPS6KB1, hereafter S6K) triggers 14-3-3 binding and inhibits mTORC2 substrate activation (Dibble et al., 2009; Treins et al., 2010). Growth factors also modulate mTOR activity through SIN1 phosphorylation at T86 and T398 (Humphrey et al., 2013; Yang et al., 2015; Liu et al., 2013). However, the phosphorylation sites in SIN1 and RICTOR identified so far appear to modify mTORC2 function globally, as opposed to influencing the activity of mTORC2 towards a particular substrate. Indeed, whether the modification state of mTORC2 subunits plays a role in dictating substrate specificity is unknown. In particular, the effect of mTORC2 subunit phosphorylation on SGK HM (S422) phosphorylation has not been addressed.

In this study, we set out to determine whether there are conditions under which mTORC2 selectively activates SGK1 but not Akt. We chose angiotensin II (AngII) as a candidate hormone for selective regulation of SGK1. AngII is a potent regulator of Na^+ balance and blood pressure homeostasis. In volume depletion, AngII stimulates the Na^+-retaining hormone aldosterone, and also directly affects salt reabsorption through regulation of ion transporters located in various segments of the kidney tubules (Herrera and Coffman, 2012). Recent evidence supports a role for SGK1 as a mediator of AngII signaling: AngII stimulates induction of SGK1 transcription (Baskin and Sayeski, 2012; Stevens et al., 2008) and knockdown of SGK1 in human proximal tubule cells impairs AngII-induced Na^+ uptake through the sodium proton exchanger 3 (NHE3) (Stevens et al., 2008). Importantly, AngII stimulates epithelial Na^+ transport in kidney tubules without affecting Akt-dependent processes such as inhibition of gluconeogenesis. Here, we find that AngII selectively triggers SGK1 S422 phosphorylation without inducing phosphorylation of Akt at either critical activating site, T308 or S473. AngII stimulates conventional PKC-dependent phosphorylation of SIN1 at S128, S315 and S356. Inhibition of conventional (c)PKC activity re-localizes SIN1 and SGK1 from the nucleus and perinuclear compartment to the plasma membrane and selectively blocks SGK1 S422 but not Akt S473 phosphorylation. Thus, we show that mTORC2 achieves specificity in signaling to SGK1 and Akt through phosphorylation of their hydrophobic motif sites at distinct cellular membranes.

RESULTS

AngII triggers selective mTORC2-dependent phosphorylation of SGK1 at its hydrophobic motif, S422

To determine whether AngII stimulates mTORC2-dependent SGK1 hydrophobic motif phosphorylation, we treated human embryonic kidney (HEK)-293T cells, expressing the angiotensin type I receptor (AT_1R, also known as AGTR1) and FLAG-tagged SGK1, with AngII either in the presence of vehicle (DMSO), an AT_1R receptor blocker (losartan) or an mTOR catalytic site inhibitor (PP242). HEK-293 cells have the machinery for AngII signaling when AT_1R is expressed (Hein et al., 1997). AngII stimulated SGK1 S422 phosphorylation and this was blocked by inhibition of AT_1R or inactivation of both mTOR complexes (PP242) (Fig. 1A). Phosphorylation of extracellular-regulated kinase 1 and 2 (ERK1/2, also known as MAPK3 and MAPK1, respectively) is a well-known consequence of AT_1R activation (Shah et al., 2004); therefore, we used ERK1/2 phosphorylation as a positive control for activation of AT_1R signaling. By comparing inhibition of mTORC1 activity (rapamycin) with total mTOR inhibition (PP242) (Fig. 1B), we found that AngII-induced SGK1 S422 phosphorylation was not blocked with rapamycin but completely prevented by PP242 suggesting that SGK1 S422 is a substrate for mTORC2 downstream of AT_1R activation. As expected, rapamycin and PP242 prevented phosphorylation of S6K, an mTORC1 target, at its hydrophobic motif, T389. In addition, we found that SGK1 S422 phosphorylation requires PI3K activity as PI3K inhibition (PIK90) prevented S422 phosphorylation (Fig. 1B). Similar to what was seen in HEK-293 cells, we found that AngII also stimulated SGK1 S422 phosphorylation predominantly through mTORC2 in the opossum proximal tubule cell line OKP (Fig. S1A) (Moe et al., 1991). Interestingly, in both HEK-293 and OKP cell lines inhibition of mTORC1 with rapamycin led to a small decrease in SGK1 S422 phosphorylation (Fig. 1B; Fig. S1A).

To further characterize the role of mTORC2 and its subunit SIN1 in regulation of AngII-induced SGK1 S422 phosphorylation, we generated HEK-293T SIN1-knockout ($SIN1^{-/-}$) cells by using CRISPR technology (Fig. 1C; Fig. S2). Consistent with our mTOR inhibitor studies, inactivation of mTORC2 by SIN1 deletion abolished both basal and AngII-stimulated SGK1 S422 phosphorylation. Reconstitution of mTORC2 activity by expression of V5-tagged wild-type SIN1 restored SGK1 S422 phosphorylation in response to AT_1R activation (Fig. 1C).

Although AngII strongly stimulated SGK1 S422 phosphorylation, surprisingly, we did not observe an increase in Akt S473 phosphorylation (Fig. 1A,C) indicating that, in response to AngII, mTORC2 targeted the HM site in SGK1 but not Akt. Note that the antibodies used to detect Akt phosphorylation cross-react with all Akt isoforms (at equivalent sites to Akt1 T308 or S473). To confirm that AngII preferentially triggers SGK1 HM phosphorylation, we directly compared AngII and insulin stimulation in $SIN1^{-/-}$ cells expressing wild-type V5-tagged SIN1 (Fig. 1D). Both AngII and insulin induced SGK1 S422 phosphorylation; however, only insulin induced Akt S473 phosphorylation. We also observed AngII-dependent SGK1 S422 phosphorylation without Akt S473 phosphorylation in OKP cells (Fig. S1A,B).

AngII stimulates PKC-dependent phosphorylation of SIN1

As a start to identifying a mechanism for distinct regulation of mTORC2-dependent SGK1 activation, we first investigated whether AngII stimulation influenced the interaction between SGK1 and SIN1. By co-immunoprecipitation experiments, we found that the amount of SGK1 associated with SIN1 did not change in response to AngII (Fig. 2A) or in response to inhibition of PI3K or mTOR activity. Instead, we observed a decrease in the mobility of SIN1 in response to AngII by performing western blotting (Fig. 2B), suggesting that SIN1 might become phosphorylated in response to this ligand. To determine whether the AngII-induced SIN1 mobility shift was due to phosphorylation, we immunoprecipitated SIN1–V5 from HEK-293-AT_1R cell extracts followed by incubation with the protein phosphatase from phage $\lambda gt10$ (Fig. 2B). HEK-293-AT_1R cells stably express HA- and Flag-tagged AT_1R (Hunyady et al.,

Journal of Cell Science (2019) 132, jcs224931. doi:10.1242/jcs.224931

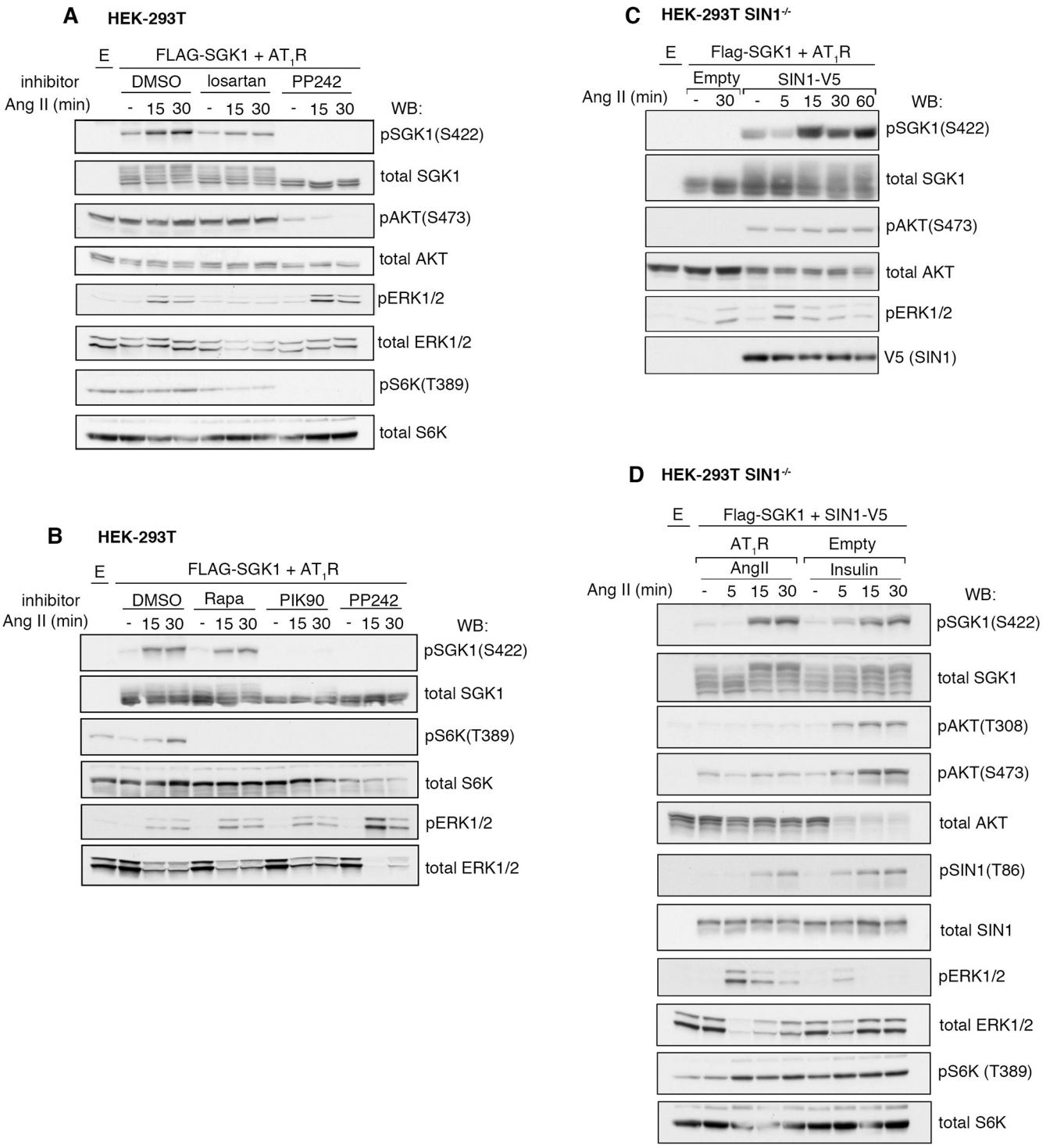

Fig. 1. AngII triggers selective mTORC2-dependent phosphorylation of SGK1 S422 in its HM. (A) Western blot (WB) analysis of whole-cell extracts (WCEs) derived from AT_1R- and Flag–SGK1-transfected HEK-293T cells that were serum starved overnight and then stimulated with 200 nM AngII for the indicated times. 10 µM losartan or 300 nM PP242 were added 15 min before AngII stimulation. DMSO was used as vehicle control. E, empty vector. (B) WB analysis of HEK-293T cells treated as in A. Inhibitors used were: 25 nM rapamycin (rapa), 1 µM PIK90 and 300 nM PP242. (C) WB analysis of WCEs derived from HEK-293T $SIN1^{-/-}$ cells transfected with Flag–SGK1 and AT_1R, and SIN1–V5 or empty vector (Empty), serum starved overnight and then stimulated with AngII for the indicated times. (D) $SIN1^{-/-}$ cells transfected as in C were serum starved overnight and then stimulated with either 200 nM AngII or 200 nM insulin for the indicated times. Results in A–D are representative of *n*=3 biological replicates. See also Figs S1 and S2.

2002). Phosphatase treatment reversed the AngII-stimulated decrease in SIN1 mobility establishing that AngII had induced phosphorylation of SIN1. In addition to PI3K and mTOR, AT_1R signaling leads to activation of various downstream mediators including PKC, protein kinase D (PKD) and ERK1/2 (Hunyady and Catt, 2006; Rozengurt, 2007). Neither PI3K nor mTOR inhibition prevented the SIN1 mobility shift (Fig. 2A), suggesting these kinases were not the AngII-induced SIN1 kinase. Next, we tried

Journal of Cell Science (2019) 132, jcs224931. doi:10.1242/jcs.224931

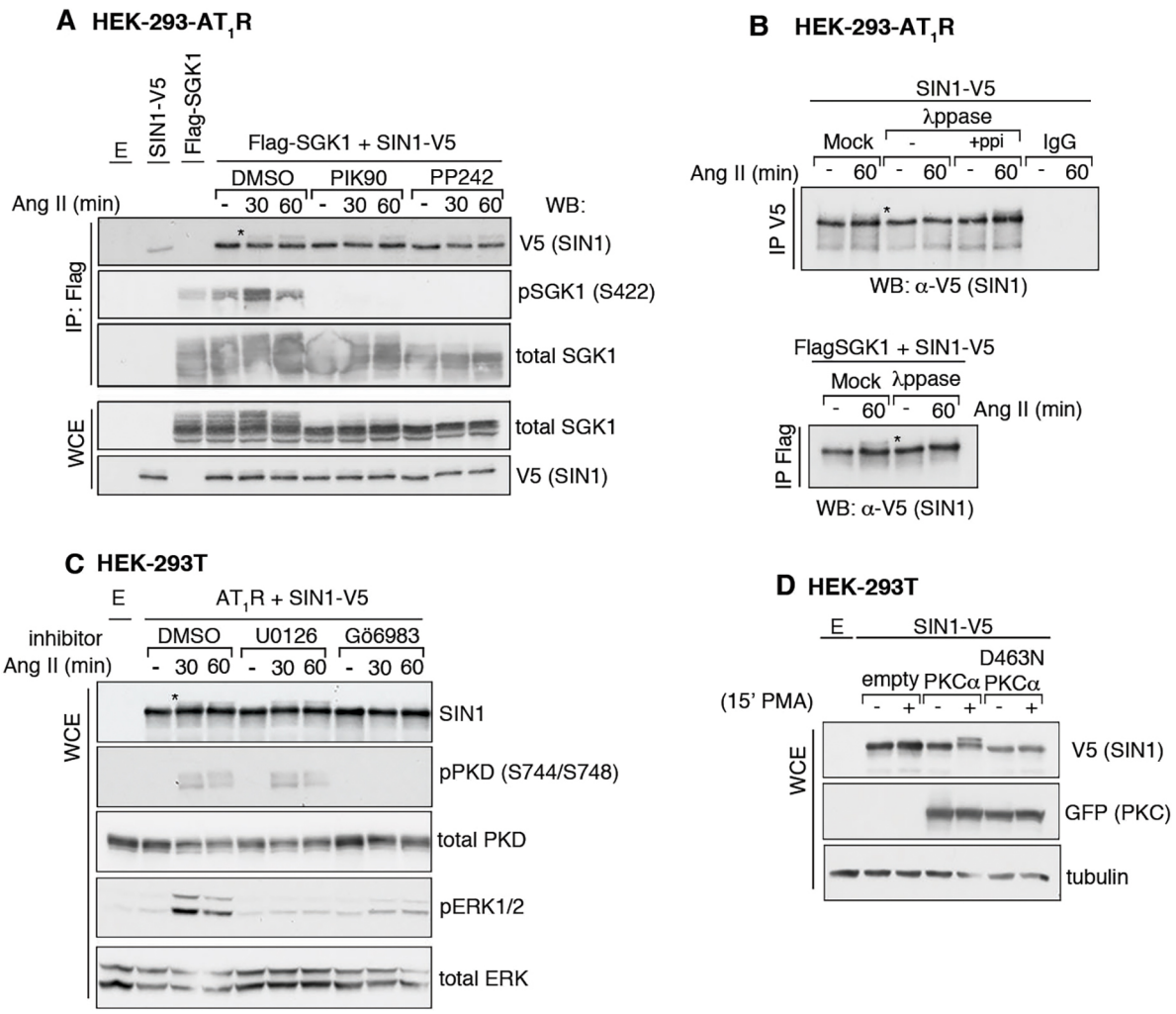

Fig. 2. AngII stimulates PKC-dependent phosphorylation of SIN1. (A) Western blot (WB) analysis of whole-cell extracts (WCEs) and Flag immunoprecipitates (IPs) derived from Flag–SGK1- and/or SIN1–V5-transfected HEK-293-AT$_1$R cells, and then serum starved overnight and stimulated with 200 nM Ang II for the indicated times. The inhibitors PIK90 (1 µM) and PP242 (300 nM) were added 15 min before addition of AngII. DMSO was used as a vehicle control. E, empty vector. Results are representative of *n*=2 biological replicates. (B) WB analysis of IPs derived from Flag–SGK1- and SIN1–V5-transfected HEK-293-AT$_1$R cells serum starved overnight and then stimulated or not for 60 min with 200 nM AngII. Top panel, SIN1 was immunoprecipitated by incubation with an anti-V5 antibody and the resuspended IPs incubated with or without λ-protein phosphatase (λ-ppase). Bottom panel, SGK1 was immunoprecipitated by incubation with Flag–agarose beads and the resuspended IPs were treated as described above with λ-ppase. A mobility shift in co-immunoprecipitated SIN1 was detected by WB analysis. The asterisk highlights the slower migrating, phosphorylated form of SIN1. Results are representative of *n*=2 biological replicates. (C) WB analysis of WCEs derived from AT$_1$R- and SIN1–V5-transfected HEK-293T cells serum starved overnight and then stimulated with 200 nM AngII for the indicated time. The inhibitors U0126 (10 µM) or Gö6983 (5 µM) were added 15 min before addition of AngII. DMSO was used as a vehicle control. E, empty vector. Results are representative of *n*=3 biological replicates. (D) WB analysis of WCEs derived from SIN1–V5 and GFP–WT PKCα or GFP–PKCα(D463N) transfected HEK-293T cells serum starved overnight and then stimulated for 15 min with 1 µM PMA. E, empty vector. Results are representative of *n*=3 biological replicates.

inhibition of ERK1/2 (via MEK inhibition with U0126) or all PKC isoforms (Gö6983) and looked for the effect of these inhibitors on the AngII-induced decreased SIN1 mobility (Fig. 2C). We found that only PKC inhibition completely prevented the AngII-induced mobility shift of SIN1. Furthermore, co-expression of SIN1 and wild-type (WT) PKCα triggered a robust mobility shift in SIN1 in response to PMA that was not observed with a kinase-dead PKCα mutant (PKCαD463N) (Fig. 2D). These results implicated PKC, most likely a conventional isoform, as a mediator of SIN1 phosphorylation in response to AngII signaling.

cPKC is required for SGK1 S422 but not Akt S473 phosphorylation

To determine whether there was a functional consequence for PKC-dependent SIN1 phosphorylation, we examined the effect of cPKC inhibition on SGK1 and Akt HM phosphorylation. Expression of the kinase-dead PKCα mutant (PKCαD463N) completely blocked SGK1 HM phosphorylation in response to AngII but had little effect on basal Akt S473 phosphorylation (Fig. 3A–C). We also assessed SIN1 T86 phosphorylation, a site that previously was shown to correlate with increased mTORC2 activity (Yang et al., 2015). AngII led to an increase in SIN1 T86 phosphorylation that was inhibited under conditions of PKCα inactivation. Consistent with these results, acute pharmacological inhibition of cPKC with LY333531 also blunted AngII-induced SGK1 S422 and SIN1 T86 phosphorylation without inhibiting Akt S473 phosphorylation (Fig. 3D–F). In addition, pretreatment with CID655763, which at 25 µM inhibits both PKD and PKC, impaired AngII-stimulated SGK1 phosphorylation (Fig. 3G). In OKP cells, PKCαD463N overexpression or acute pharmacological inhibition

Journal of Cell Science (2019) 132, jcs224931. doi:10.1242/jcs.224931

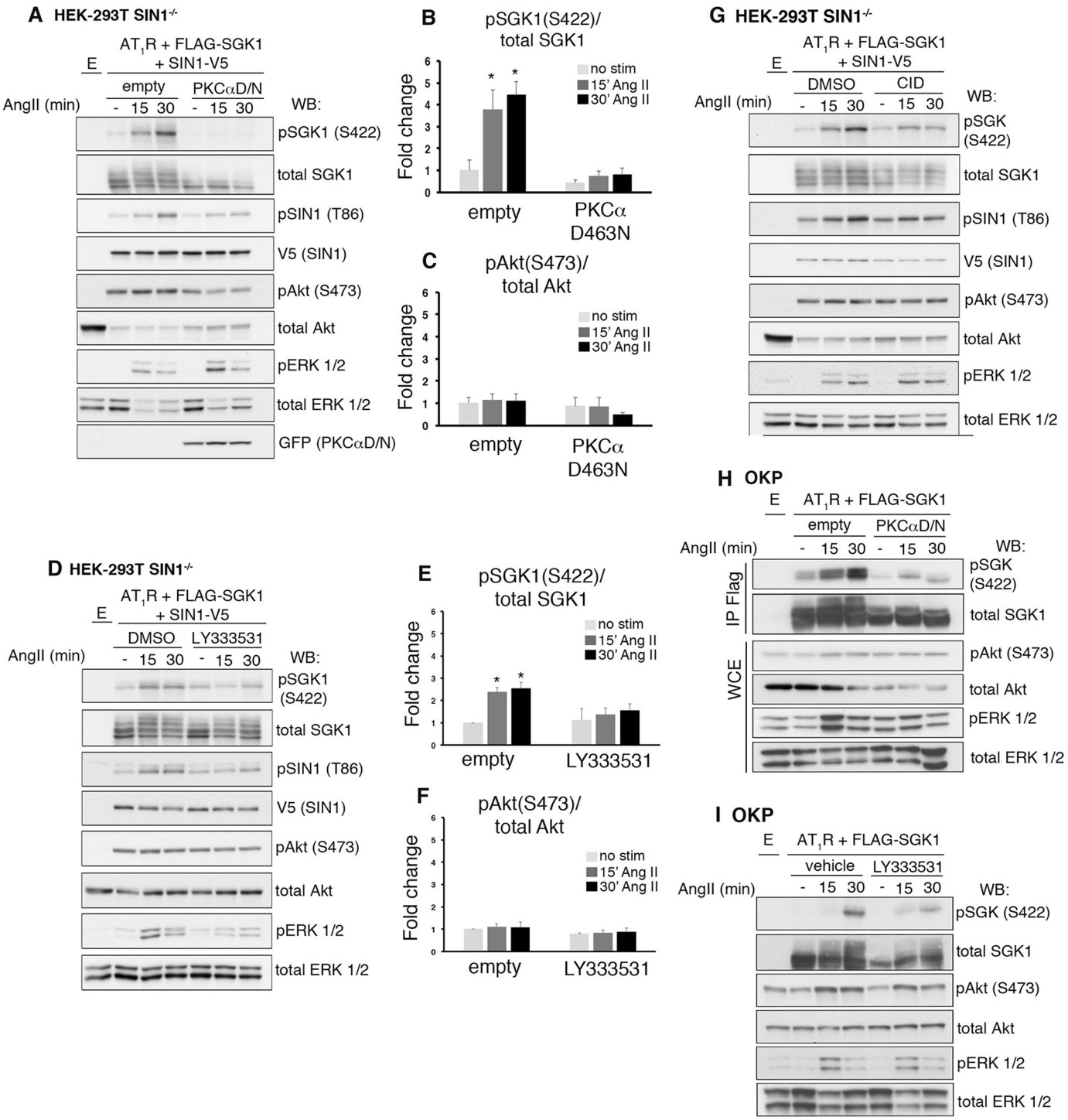

Fig. 3. PKC activity is required for AngII-induced SGK1 S422 phosphorylation. (A) Western blot (WB) analysis of whole-cell extracts (WCEs) derived from SIN1$^{-/-}$ cells transfected with AT$_1$R, Flag–SGK1 and SIN1–V5, and GFP–PKCα(D463N) or empty vector (empty) as indicated. E, empty vector. Cells were serum starved overnight before treatment with 200 nM AngII for the times shown. Results are representative of *n*=3 biological replicates. (B,C) Quantification of WBs as in A for pSGK1(S422) and pAkt(S473), corrected to total protein level; values represent fold change from the results with unstimulated empty vector. Data are represented as mean±s.e.m. **P*<0.05 for unstimulated versus AngII (Student's *t*-test). (D) WB analysis of WCEs derived from SIN1$^{-/-}$ cells transfected with AT$_1$R, Flag–SGK1 and SIN1–V5. Cells were serum starved overnight before treatment with 200 nM AngII for the times shown. Where indicated, the cPKC inhibitor, LY333531, was added. Results are representative of *n*=3 biological replicates. (E,F) Quantification of pSGK1(S422) and pAkt(S473) WBs as in D, corrected to total protein level; values represent fold change from unstimulated empty vector. Data are represented as mean±s.e.m. **P*<0.05 for unstimulated versus AngII (Student's *t*-test). (G) WB analysis of WCEs derived from SIN1$^{-/-}$ cells transfected with AT$_1$R, Flag–SGK1 and SIN1–V5. Cells were serum starved overnight before treatment with 200 nM AngII. Where indicated, the PKD inhibitor CID655763 was added. Results are representative of *n*=2 biological replicates. (H) WB analysis of WCEs derived from OKP cells transfected with AT$_1$R, Flag–SGK1, and GFP–PKCαD463N or empty vector (empty) as indicated. Cells were serum starved overnight before treatment with 200 nM AngII for the times shown. Results are representative of *n*=2 biological replicates. (I) WB analysis of WCEs derived from OKP cells transfected with AT$_1$R and Flag–SGK1 (E, empty vector). Cells were serum starved overnight before treatment with 200 nM AngII for the times shown. Where indicated, the cPKC inhibitor LY333531 was added. Results are representative of *n*=2 biological replicates.

Journal of Cell Science (2019) 132, jcs224931. doi:10.1242/jcs.224931

of cPKC also blocked AngII-induced SGK1 S422 phosphorylation (Fig. 3H,I). To determine whether the effect of PKC on mTORC2-dependent SGK1 activation was selective for AT_1R signaling or a more general requirement for SGK1 activation, we examined the effect of PKC inactivation on insulin-stimulated SGK1 and Akt HM phosphorylation. Similar to AT_1R signaling, when PKCα kinase activity was disrupted either by expression of PKCαD463N or pre-treatment with LY333531, SGK1 S422 phosphorylation was markedly reduced in response to insulin compared to control (Fig. 4A,B). In striking contrast, insulin-stimulated Akt S473 phosphorylation was not significantly altered with PKCα kinase inactivation (Fig. 4A,B). Similar results were obtained in mouse embryonic fibroblasts (MEFs) and OKP cells transfected with PKCαD463N and Flag–SGK1 (Fig. 4C,D). Combined, these results suggest that cPKC activity is a general requirement for SGK1 S422 phosphorylation and, importantly, that Akt S473 phosphorylation occurs through a distinct mechanism.

cPKC and PKD induce phosphorylation of SIN1 at S128, S315 and S356

The results described above are consistent with a role for PKC-mediated phosphorylation of SIN1 in regulation of SGK1 S422 phosphorylation. To identify the site(s) of PKC-mediated phosphorylation on SIN1, we performed mass spectrometry on SIN1 immunoprecipitated from HEK-293T cell extracts overexpressing Flag-tagged SIN1 and either WT PKCα or PKCαD463N and stimulated with phorbol 12-myristate 13-acetate (PMA). We observed three serine residues, S128, S315 and S356 (mouse sequence), whose phospho-occupancy increased in the presence of WT PKCα but not with the catalytically inactive PKCαD463N (Fig. 5A; Figs S3, S4A, S5 and Tables S1 and S2). We compared these results to those obtained when SIN1–Flag was immunoprecipitated from extracts of HEK-293 cells expressing AT_1R stimulated with AngII, in the presence or absence of PKC inhibition (Gö6983) (Fig. 5B; Figs S3, S4B, S5 and Tables S1 and

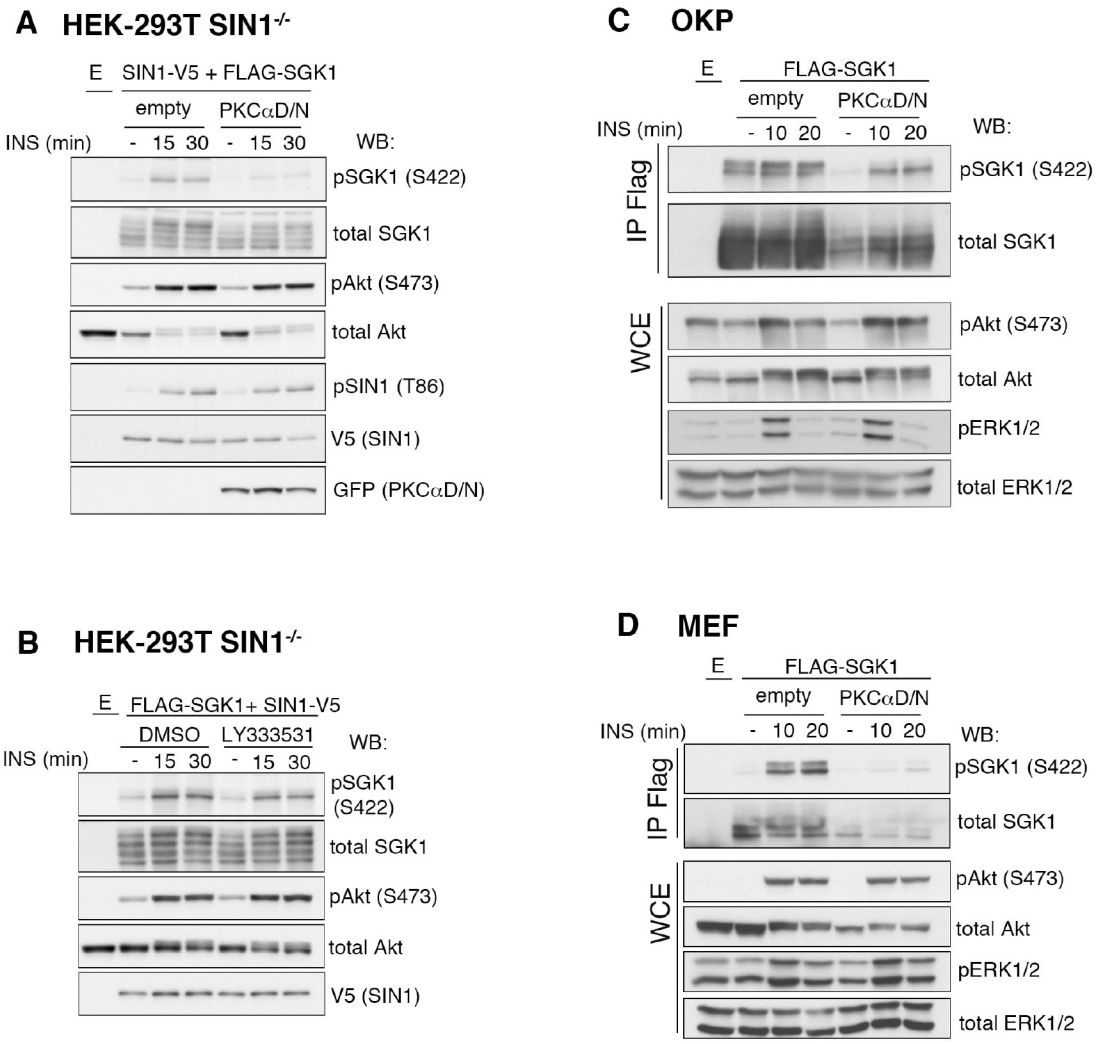

Fig. 4. Insulin-stimulated SGK1 S422 phosphorylation but not Akt S473 phosphorylation requires PKC activity. (A) Western blot (WB) analysis of whole-cell extracts (WCEs) from $SIN1^{-/-}$ cells transfected with Flag–SGK1, SIN1–V5 and GFP–PKCα(D463N) or empty vector (empty) as indicated. E, empty vector. Cells were serum starved overnight before treatment with 200 nM insulin (INS) for the times shown. Results are representative of *n*=3 biological replicates. (B) WB analysis of WCEs derived from $SIN1^{-/-}$ cells transfected with Flag–SGK1 and SIN1–V5. Cells were serum starved overnight before treatment with 200 nM insulin for the times shown. Where indicated, the cPKC inhibitor LY333531 was added. (C) WB analysis of WCEs derived from OKP cells transfected with Flag–SGK1 and GFP–PKCα(D463N) or empty vector as indicated. Cells were serum starved overnight before treatment with 200 nM insulin for the times shown. (D) WB analysis of WCEs derived from WT MEFs transfected with Flag–SGK1 and GFP–PKCα(D463N) or empty vector as indicated. Cells were serum starved overnight before treatment with 200 nM insulin for the times shown. Results in B–D are representative of *n*=2 biological replicates.

Journal of Cell Science (2019) 132, jcs224931. doi:10.1242/jcs.224931

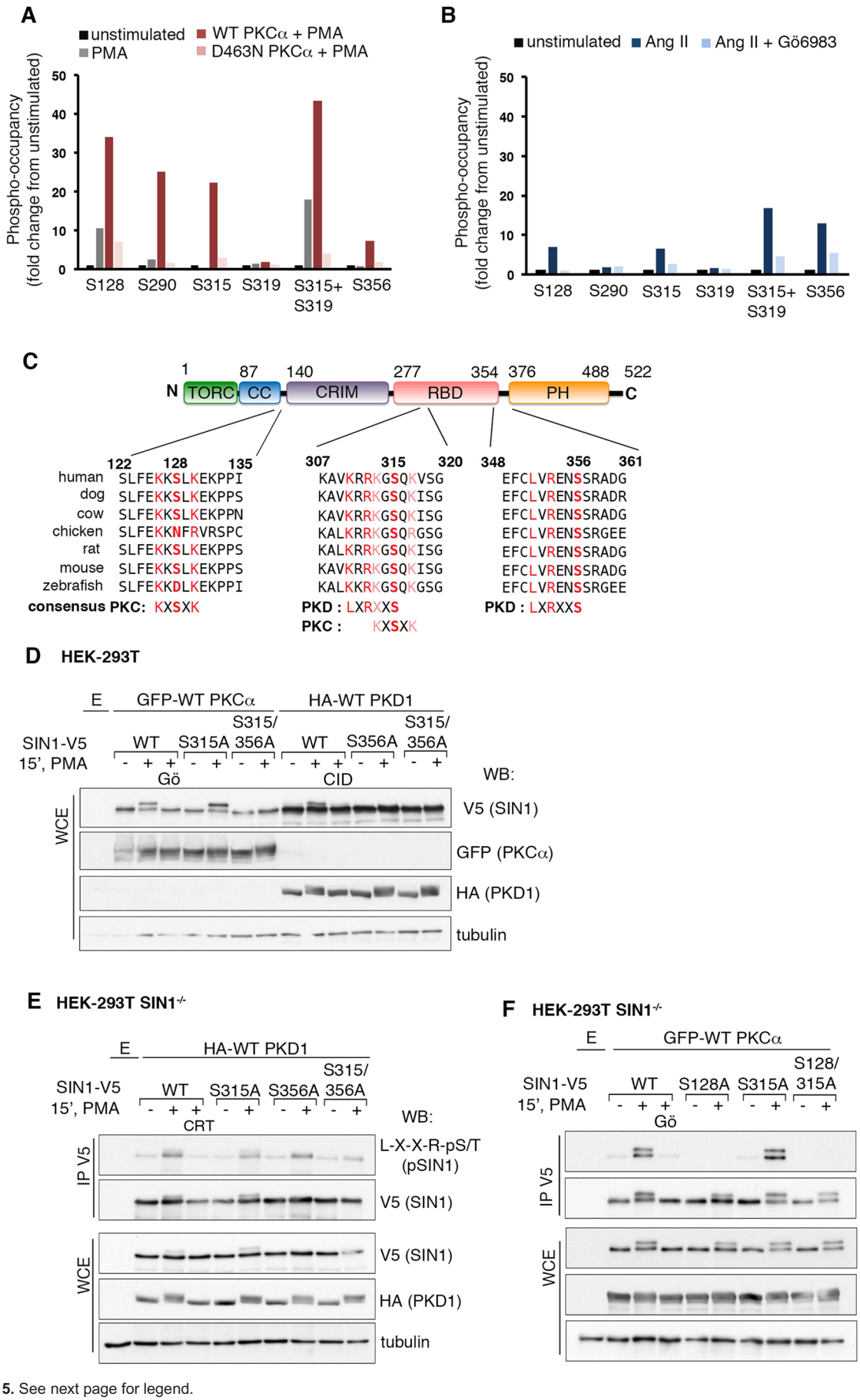

Fig. 5. See next page for legend.

Journal of Cell Science (2019) 132, jcs224931. doi:10.1242/jcs.224931

Fig. 5. PKC and PKD induce phosphorylation of SIN1 at S128, S315 and S356. (A) Relative quantification of phosphopeptide abundance. HEK-293 cells were transfected with WT SIN1–Flag, and either WT PKCα or GFP–PKCαD463N. Cells were stimulated with 1 µM PMA for 15 min as indicated. Results are representative of *n*=3 biological replicates. (B) Relative quantification of phosphopeptide abundance. HEK-293-AT_1R cells were transfected with empty vector or SIN1–Flag followed by stimulation with 200 nM AngII either in the presence of vehicle (DMSO) or the PKC inhibitor Gö6983 (5 µM) for 60 min. Both graphs show MS results for SIN1–Flag trypsin digestion. Results are in A and B show a representative of *n*=3 biological replicates. See also Figs S3, S4, S5 and Tables S1 and S2. (C) SIN1 domain structure and sequence of the regions surrounding S128, S315 and S356. TORC, putative mTOR-binding domain; CC, coiled-coil domain; CRIM, conserved region in the middle domain; RBD, Raf-like Ras-binding domain; PH, pleckstrin homology domain. (D) Western blot (WB) analysis of whole-cell extracts (WCEs) derived from HEK-293T cells transfected with GFP-tagged WT PKCα or HA-tagged WT PKD1 and the indicated SIN1–V5 constructs. Cells were serum starved overnight and then stimulated for 15 min with 1 µM PMA in the presence of vehicle (DMSO) or the indicated inhibitors [5 µM Gö6976 (Gö) or 25 µM CID655763 (CID)]. (E) WB analysis of WCEs and anti-V5 immunoprecipitations (IPs) derived from $SIN1^{-/-}$ cells transfected with WT HA–PKD1 and the indicated SIN1–V5 constructs. Cells were serum starved overnight before stimulating with 1 µM PMA for 15 min either in the presence of vehicle (DMSO) or 5 µM CRT0066101 (CRT). (F) WB analysis of WCE and anti-V5 IPs derived from $SIN1^{-/-}$ cells transfected with WT GFP–PKCα and the indicated SIN1–V5 constructs. Cells were treated as in E except the inhibitor, 5µM Gö6976 D(Gö), was added where indicated. See also Fig. S6. Results are in D–F are representative of *n*=2 biological replicates.

S2). In both mass spectrometry experiments, the same three residues were reproducibly identified. S128 is in a canonical PKC recognition motif (K-x-S/T-x-K) and is located between the coiled-coiled (CC) and conserved region in the middle (CRIM) domains in the N-terminus of SIN1. The sequence surrounding S356 is a strong PKD recognition motif (L-x-x-R-S/T) and is found between the Raf-like Ras-binding (RBD) and the pleckstrin homology (PH) domains. The S315 site has characteristics of both PKC and PKD recognition motifs and is located within the RBD. All three residues are conserved in vertebrates (Fig. 5C). In support of our mass spectrometry data, overexpression of PKD led to a similar decrease in SIN1 mobility because PKCα overexpression and the decreased SIN1 mobility was completely blocked by PKD inhibition upon CID755673 treatment (Fig. S6A). G-protein-coupled receptors (GPCRs) and receptor tyrosine kinases (RTKs) activate PKD via two mechanisms: (1) binding to the second messenger diacylglycerol (DAG) followed by (2) conventional or novel PKC phosphorylation at the activation loop and autophosphorylation at the C-terminus (Steinberg, 2012). Consistent with PKD requiring activation by cPKC, co-expression of PKD with PKCαD463N, prevented the SIN1 mobility shift (Fig. S6B). Since overexpression of PKD was sufficient to induce the SIN1 mobility shift (Fig. S6A), we speculated that phosphorylation of a PKD consensus motif at S315 or S356 was likely to cause the delayed SIN1 mobility. To answer this question, we co-expressed PKCα or PKD1 with WT SIN1–V5 or the non-phosphorylatable SIN1 alanine mutants S315A, S356A or the double mutant S315A/S356A. PMA treatment triggered the delay in SIN1 mobility when WT or the S315A SIN1–V5 was expressed. In contrast, decreased SIN1 mobility was not observed when S356A or S315A/S356A SIN1–V5 was expressed (Fig. 5D), indicating that S356 phosphorylation is required for the observed SIN1 mobility shift.

AngII and insulin signaling trigger phosphorylation of SIN1 at S128 by PKC

To confirm phosphorylation of SIN1 by PKD at S356 and to determine whether the other sites identified by mass spectrometry were phosphorylated in response to PKC or PKD, we examined SIN1 phosphorylation induced by expression of PKC or PKD with anti-PKC or anti-PKD phospho-substrate antibodies. When PKD and WT SIN1–V5 were co-transfected in $SIN1^{-/-}$ cells, PMA stimulated SIN1 phosphorylation (as detected by an anti-L-x-x-R-pS/T antibody) and this phosphorylation was prevented by PKD inhibition with CRT0066101 (a specific PKD inhibitor) (Fig. 5E). Mutation of S356 to alanine (S356A) alone did not prevent SIN1 phosphorylation suggesting another site on SIN1 was also phosphorylated by PKD (Fig. 5E). Accordingly, when $SIN1^{-/-}$ cells were reconstituted with S315A SIN1, phosphorylation of SIN1 in response to PMA was reduced. Expression of the S315A/S356A double alanine mutant reduced SIN1 phosphorylation further, suggesting that PKD phosphorylates SIN1 at both the S315 and S356 sites (Fig. 5E). We also assessed phosphorylation of SIN1 by PKC using an anti-R/K-x-pS-x-R/K (pPKC substrate) antibody. Treatment of $SIN1^{-/-}$ cells expressing both PKCα and WT SIN1 with PMA induced phosphorylation of SIN1 and this phosphorylation was blocked by PKC inhibition with Gö6976 (which blocks the activity of conventional PKC isoforms) (Fig. 5F). In $SIN1^{-/-}$ cells reconstituted with the S128A SIN1 mutant, PMA-induced PKC phosphorylation was completely blocked, whereas expression of the S315A mutant exhibited comparable phosphorylation to WT SIN1. This suggests that PKC phosphorylates SIN1 exclusively at S128 and demonstrates the specificity of this antibody for SIN1 phosphorylated at this residue. Thus, based on peptide sequence data and western blot analysis, it is likely that PKC directly phosphorylates SIN1 at S128 and indirectly regulates phosphorylation at S315 and S356 through activation of PKD.

We next determined whether AngII or insulin signaling induces phosphorylation of SIN1 by using the anti-R/K-x-pS-x-R/K antibody which, as was shown in Fig. 5F, recognizes phosphorylation at S128. SIN1 S128 phosphorylation was observed at 5, 15, 30 and 60 min post-AngII stimulation (Fig. 6A). To assess whether cPKC activity was required for AngII-induced SIN1 phosphorylation we co-treated cells with both AngII and LY333531. LY333531 completely prevented the AngII-induced SIN1 S128 phosphorylation. Insulin also stimulated SIN1 S128 phosphorylation (Fig. 6B). Insulin-stimulated SIN1 phosphorylation peaked at 15 min post-treatment and, similar to AngII, was prevented by inhibition of cPKC. Thus, both AngII and insulin treatment elicit cPKC-dependent SIN1 phosphorylation at S128. It is notable that the AngII-induced SIN1 phosphorylation is more sustained than that induced by insulin.

cPKC-dependent SIN1 S128 phosphorylation is not required for SGK1 S422 phosphorylation

As PKC-dependent SIN1 phosphorylation occurred on a timescale consistent with regulation of mTORC2-dependent SGK1 HM phosphorylation, we hypothesized that PKC-induced SIN1 phosphorylation might be required for AngII-stimulated SGK1 activity. To determine whether PKC exerts its effects on SGK1 HM phosphorylation directly through phosphorylation of SIN1, we examined SGK1 phosphorylation in $SIN1^{-/-}$ cells reconstituted with WT SIN1, SIN1 with a non-phosphorylatable serine-to-alanine mutation (S128A) or a phospho-mimetic serine-to-aspartate mutation (S128D). We initially focused on the PKC consensus site, S128, since specific inhibition of PKD activity with CRT0066101 did not prevent AngII-induced SGK1 S422 phosphorylation (data not shown). Surprisingly, we observed a similar increase in AngII-stimulated SGK1 S422 phosphorylation when $SIN1^{-/-}$ cells were reconstituted with either the S128A or

Journal of Cell Science (2019) 132, jcs224931. doi:10.1242/jcs.224931

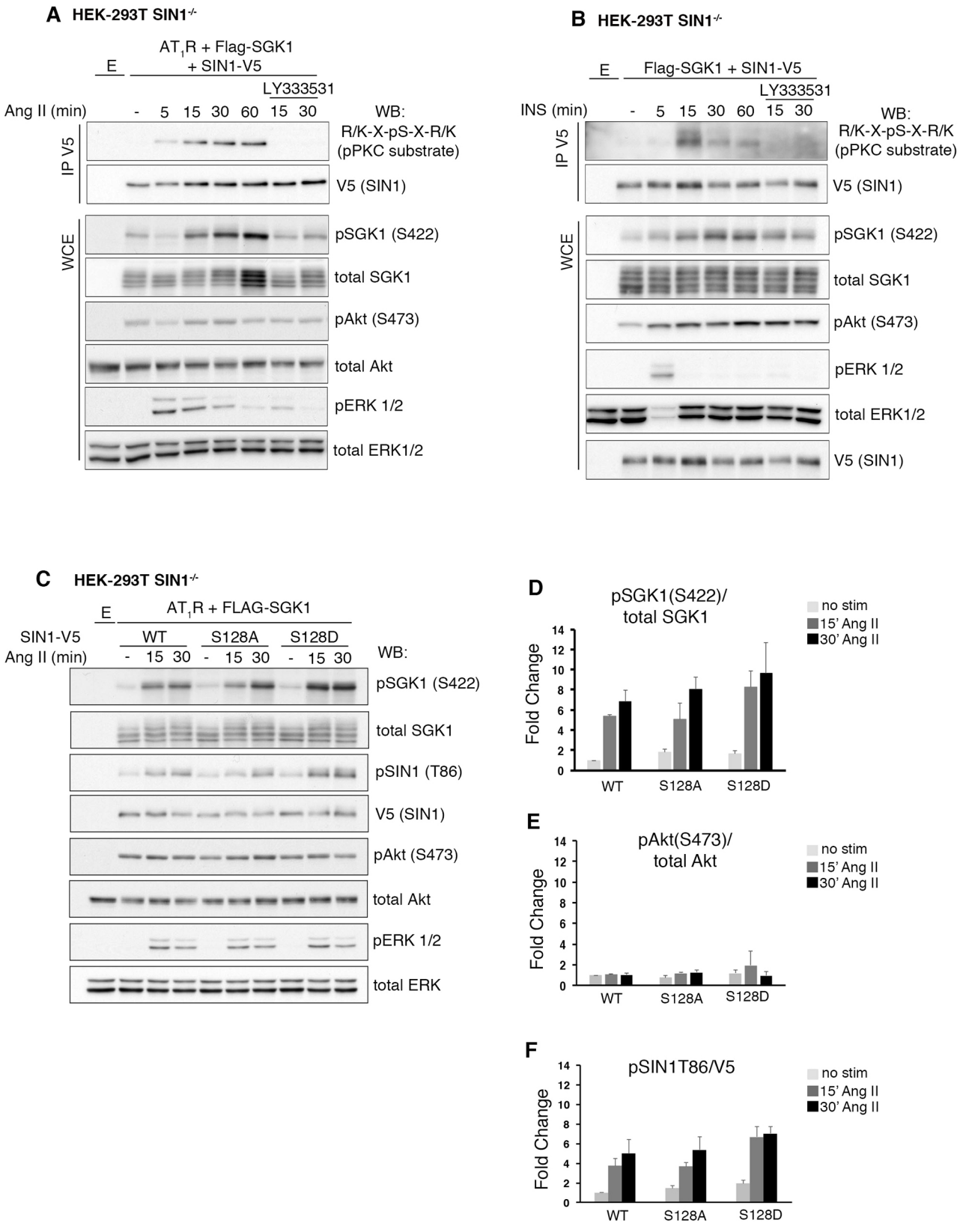

Fig. 6. See next page for legend.

S128D SIN1 mutant (Fig. 6C–F). We found similar results for SGK1 S422 phosphorylation in SIN1$^{-/-}$ cells reconstituted with triple alanine (S128/S315/S356A) or aspartate (S128/S315/S356D) SIN1 mutants (data not shown). Thus, cPKC-dependent phosphorylation of SIN1 does not play a primary role in regulation of SGK1 S422 phosphorylation and is not the mechanism underlying inhibition of SGK1 S422 phosphorylation upon PKC inactivation.

Journal of Cell Science (2019) 132, jcs224931. doi:10.1242/jcs.224931

Fig. 6. AngII and insulin signaling trigger phosphorylation of SIN1 at S128 but SIN1 S128 phosphorylation is not required for SGK1 S422 phosphorylation. (A) Western blot (WB) analysis of whole-cell extracts (WCEs) and anti-V5 immunoprecipitations (IPs) derived from SIN1$^{-/-}$ cells transfected with Flag–SGK1, SIN1–V5 and AT_1R. Cells were serum starved overnight before treating with AngII (200 nM) for the times shown. Where indicated, the cPKC inhibitor LY333531 (200 nM), was added. E, empty vector. (B) WB analysis of WCEs and anti-V5 IPs derived from SIN1$^{-/-}$ cells transfected with Flag–SGK1, SIN1–V5 and empty vector. Cells were serum starved overnight before treating with insulin (INS) (200 nM) for the times shown. Where indicated, the cPKC inhibitor LY333531 was added. Results are in A and B show a representative of *n*=2 biological replicates. (C) WB analysis of WCEs derived from SIN1$^{-/-}$ cells transfected with AT_1R, Flag–SGK1 and the indicated SIN1–V5 constructs. Cells were serum starved overnight and then treated with AngII (200 nM) for the times shown. Results are representative of *n*=3 biological replicates. (D–F) Quantification of pSGK1 S422, pAkt S473 and pSIN1 T86 levels from WBs as shown in C, corrected for total protein level; values represent fold change from unstimulated 'WT SIN1'. Data are represented as mean±s.e.m. (*n*=3 biological replicates).

Inhibition of cPKC catalytic activity disrupts SIN1 and SGK1 subcellular localization

cPKCs have been implicated in the spatial control of signal transduction in cells due to coupling of their membrane binding with kinase activation (Rosse et al., 2010). Importantly, the CRIM domain within SIN1 directly binds mTORC2 targets from the AGC kinase family, including PKC, SGK1 and Akt (Cameron et al., 2011; Lu et al., 2011; Tatebe et al., 2017). Previously, PKCα was implicated in mediating the localization of SIN1, RICTOR and mLST8 with syndecan-4 in lipid rafts of endothelial cells, which is required for proper growth-factor-induced Akt S473 phosphorylation (Partovian et al., 2008). Therefore, we asked whether cPKC activation controls SIN1 and SGK1 subcellular localization in HEK-293 cells and thereby influences SGK1 S422 phosphorylation. Through indirect immunofluorescence and confocal microscopy, we found that, in serum-starved SIN1$^{-/-}$ cells reconstituted with WT SIN1–V5, SIN1 was localized prominently to the nucleus and to a lesser extent to the cytoplasm and plasma membrane. Activation of exogenously expressed WT PKCα with PMA led to the re-localization of SIN1 from the nucleus to a perinuclear compartment, the cytoplasm and the plasma membrane (Fig. S7). Stimulation of HEK-293-AT_1R cells with AngII also led to redistribution of exogenously expressed SIN1–V5 and Flag–SGK1 from the nucleoplasm to the cytoplasm and the plasma membrane (Fig. 7A,D). Strikingly, in serum-starved cells expressing GFP–PKCαD463N, nuclear localization of SIN1–V5 and Flag–SGK1 was significantly reduced and both proteins were found prominently localized at the plasma membrane (Fig. 7C,F; Fig. S8). Stimulation of these cells with AngII or insulin did not alter the localization of SIN1–V5 or Flag–SGK1 further. RICTOR was also re-localized from the cytoplasm to the plasma membrane in serum-starved cells when co-expressed with SIN1 and PKCαD463N (Fig. 8A). However, when mTOR was co-expressed with SIN1 and PKCαD463N, only a fraction of mTOR re-localized to the plasma membrane, consistent with the existence of two mTOR complexes (Fig. 8B). Interestingly, it has been reported that inhibition of cPKC catalytic activity causes pre-targeting of the inactive protein to the plasma membrane and accelerated agonist-induced translocation compared to that observed for WT PKC (Antal et al., 2014). We also observed reduced SIN1 and SGK1 localization in the nucleoplasm when cPKC activity was inhibited with LY333531, although the plasma membrane targeting was less-pronounced than with overexpression of PKCαD463N (Fig. 7B,E). Collectively, these data suggest that cPKC activation by PMA or AngII triggers the redistribution of SIN1 and SGK1 from a predominantly nuclear localization to a perinuclear compartment, cytoplasm and plasma membrane. However, premature re-localization of SIN1 and SGK1 away from the nucleus or perinuclear compartment through inhibition of cPKC catalytic activity selectively prevents SGK1 S422 but not Akt S473 phosphorylation and is consistent with a model where mTORC2 target specificity is achieved through subcellular partitioning of mTORC2 activity.

DISCUSSION

How pleiotropic master signaling molecules, such as mTOR, receive specific signaling inputs and respond selectively to modulate distinct physiological processes represents a general problem in signaling biology. In this report, we show that the highly related but functionally distinct kinases, SGK1 and Akt are phosphorylated by mTORC2 at different cellular membranes. cPKC, a critical downstream mediator of AT_1R signaling, regulates SIN1 and SGK1 subcellular localization. Inhibition of cPKC catalytic activity leads to re-localization of SIN1 and SGK1 from nuclear and peri-nuclear subcellular domains to the plasma membrane and inhibits SGK1, but not Akt, HM phosphorylation. Collectively, our results demonstrate that mTORC2-dependent SGK1 phosphorylation occurs at a perinuclear compartment, not the plasma membrane, and suggests that mTORC2 achieves specificity in SGK1 and Akt activation through phosphorylation of their hydrophobic motif sites at distinct subcellular locations.

AngII, a primary component of the renin–angiotensin–aldosterone system (RAAS), is responsible for the physiological control of blood pressure, thirst and Na^+ balance (Hunyady and Catt, 2006). The physiological and pathophysiological actions of AngII are predominantly mediated via activation of the AT_1R, a typical seven-transmembrane GPCR. In response to AngII, AT_1R couples primarily through $G_{q/11}$-mediated inositol phosphate/Ca^{2+} signaling (Hunyady and Catt, 2006). Through both pharmacological and genetic means, we demonstrate that AngII signaling triggers SGK1 S422 phosphorylation through mTORC2, not mTORC1, activity. AngII signaling can in some cases trigger transactivation of growth factor receptor tyrosine kinases (RTKs) and induce Akt S473 phosphorylation (Higuchi et al., 2007; Daub et al., 1996). However, this cross-communication does not occur in HEK-293T cells (Higuchi et al., 2007; Hunyady and Catt, 2006; Shah et al., 2004). Surprisingly, we find that RTK-independent AT_1R activation does not trigger phosphorylation of Akt S473 despite mTORC2 activation and phosphorylation of SGK1 at its comparable HM site, S422. It is now known that many GPCRs generate signals from intracellular compartments, including the nucleus, ER and endosomes (Irannejad et al., 2015). AT_1R has been shown to undergo AngII-mediated internalization and translocation to the nucleus and endosomes (Hunyady and Catt, 2006; Lu et al., 1998). Thus, activation of AT_1R signaling at a localized domain, such as the nucleus, ER or mitochondria-associated ER membranes (MAMs), could underlie the specificity in AngII activation of SGK1 in HEK-293T and OKP cells.

How mTORC2 activation is regulated and why mTORC2 is localized to various subcellular compartments are major unanswered questions in the mTOR signaling field. Several mechanisms for mTORC2 activation have been proposed which include binding of the complex to ribosomes (Zinzalla et al., 2011), interaction of mTOR with the small GTPase Rac1 (Saci et al., 2011) and binding of the complex to PIP_3 at the plasma membrane through the PH domain of SIN1 (Gan et al., 2011; Liu et al., 2015b). In addition, post-

Journal of Cell Science (2019) 132, jcs224931. doi:10.1242/jcs.224931

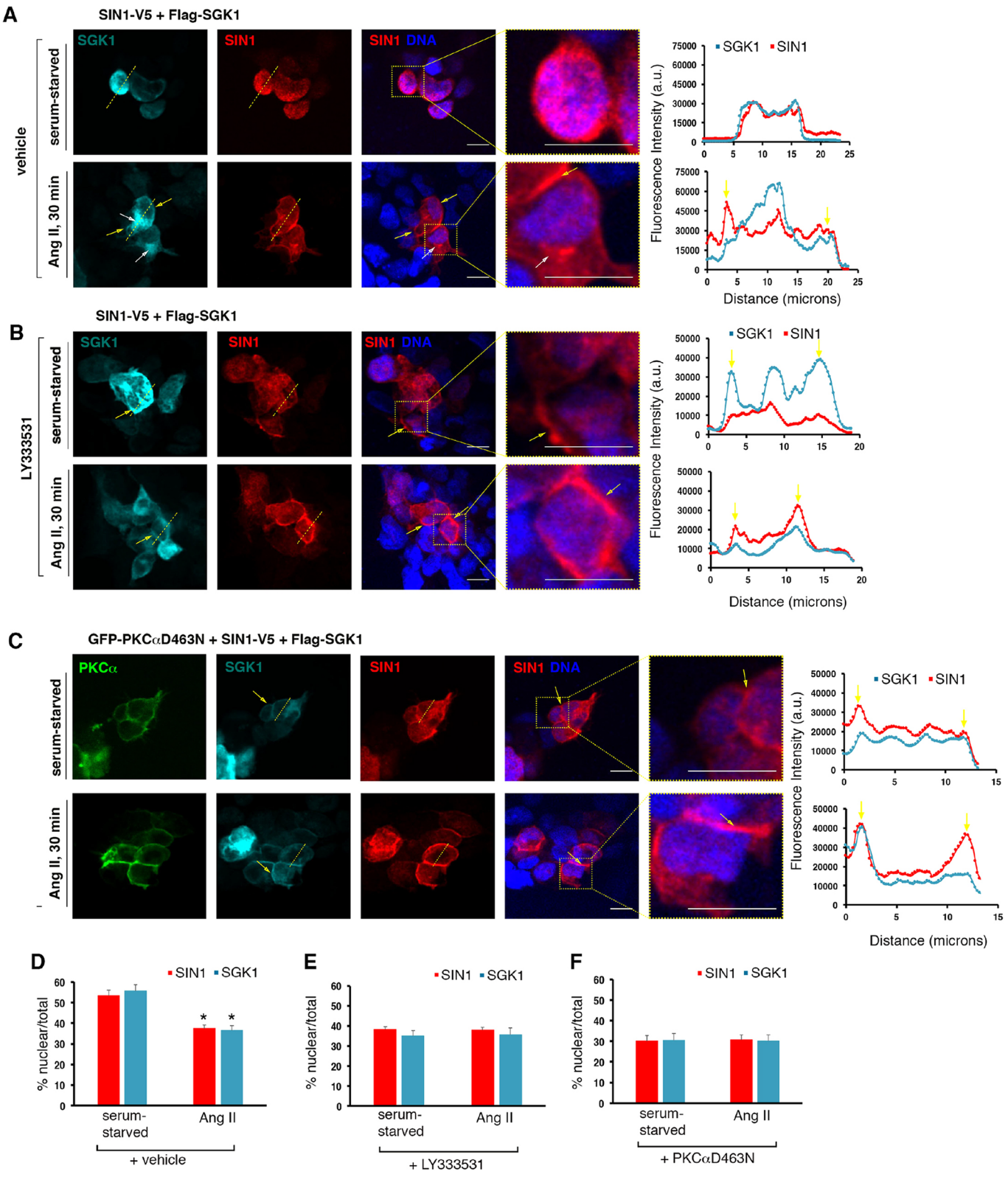

Fig. 7. See next page for legend.

translational modifications such as acetylation and phosphorylation of mTORC2 subunits have been shown to modulate mTOR activity (Gaubitz et al., 2016; Humphrey et al., 2013; Liu et al., 2013; Yang et al., 2015). In this study, we identify three serine residues on SIN1 (S128, S315 and S356) that are phosphorylated in response to cPKC activation. However, we find that SIN1 phosphorylation at these sites is not required for AngII-induced SGK1 S422 or Akt S473 phosphorylation. We do observe a trend for enhanced SIN1 T86 and SGK1 S422 phosphorylation in response to AngII when SIN1$^{-/-}$ cells are reconstituted with the phospho-mimetic (S128D) SIN1

Journal of Cell Science

Journal of Cell Science (2019) 132, jcs224931. doi:10.1242/jcs.224931

Fig. 7. Inhibition of cPKC catalytic activity disrupts SIN1 and SGK1 subcellular localization. (A) HEK-293-AT$_1$R cells expressing SIN1–V5 and Flag–SGK1 were serum starved overnight and either left unstimulated or stimulated with AngII for 30 min. Cells were then processed in an immunofluorescence assay to detect SGK1 and SIN1, and co-stained with DAPI to detect nuclei and imaged through confocal microscopy. Representative individual SGK1 and SIN1 line scans (from the line shown in left two panels) are shown on the right. (B) HEK-293-AT$_1$R cells expressing SIN1–V5 and Flag–SGK1 were serum starved overnight and then in the presence of LY333531 were either stimulated with AngII for 30 min or left unstimulated. Representative individual SGK1 and SIN1 line scans (from the line shown in left two panels) are shown on the right. (C) HEK-293AT$_1$R cells expressing SIN1–V5, FLAG–SGK1 and PKCαD436N were treated as in A. Representative individual SGK1 and SIN1 line scans (from the line shown in left two panels) are shown on the right. (D–F) Quantification of SIN1 and SGK1 nuclear localization as a percentage of total SIN1 or SGK1 staining for experiments with vehicle, LY333531 and GFP–PKCαD463N, respectively. Data are represented as mean±s.e.m. *P<0.05, unstimulated versus AngII (Student's t-test). (D) SIN1, n=3 biological replicates, SGK1, n=2 biological replicates; SIN1 serum-starved n=55 cells, Ang II n=75 cells; SGK1 serum-starved n=26 cells, Ang II n=23 cells. (E) SIN1, n=2 biological replicates, SGK1, n=2 biological replicates; SIN1 serum-starved n=29 cells, Ang II, n=35 cells; SGK1 serum-starved n=22 cells, Ang II n=32 cells. (F) SIN1, n=2 biological replicates, SGK1, n=2 biological replicates; SIN1 serum-starved n=35 cells, Ang II n=42 cells; SGK1 serum-starved n=37 cells, Ang II n=29 cells. White arrows indicate peri-nuclear staining and yellow arrows (in both images and line scans) indicate plasma membrane localization. Scale bars: 10 µm. See also Figs S7 and S8.

mutant. Notably, no trend was observed for Akt S473 phosphorylation. As SIN1 T86 phosphorylation has been reported to enhance growth factor-stimulated mTORC2 activity towards Akt (Yang et al., 2015), it is possible that AngII-induced phosphorylation of SIN1 at S128 facilitates phosphorylation at SIN1 T86 to potentiate SGK1-associated mTORC2 activity towards SGK1. Future work is needed to determine the precise role for PKC-mediated SIN1 phosphorylation.

SIN1 is the only mTORC2 subunit that contains a lipid-binding domain and has been shown to target mTORC2 to cellular membranes (Ebner et al., 2017; Liu et al., 2015a). mTORC2 has been detected in the cytosol, nucleus, early and late endosomes and plasma membrane in various cell lines including HEK-293T cells (Betz and Hall, 2013; Ebner et al., 2017). Interestingly, a recent study has shown that SIN1 subcellular localization does not change in response to growth factor stimulation or PI3K inhibition, suggesting that SIN1 interacts with cellular membranes independently of phosphatidylinositol (3,4,5)-trisphosphate (PIP_3) (Ebner et al., 2017). Here, we detect a similar pattern of SIN1 localization and also observe that SIN1 localization does not markedly change in response to insulin stimulation (Fig. S8). However, we find that PMA-activated PKCα and AT$_1$R signaling, which strongly activates PKC, induces translocation of SIN1 and SGK1 from the nucleus to the cytosol, perinuclear membranes and plasma membrane. The relocation of SIN1 from the nucleus to cellular membranes in response to AT$_1$R signaling suggests that mTORC2 localization is uniquely regulated in response to growth factor- or GPCR-stimulated signaling pathways.

While there is compelling evidence that the PH domain of SIN1 can target mTORC2 to the plasma membrane and other cellular membranes, we (this study) and another group have demonstrated that PKCα plays an important role in the subcellular localization of SIN1 and RICTOR (Partovian et al., 2008). Partovian et al. reported that in syndecan-4-deficient mice, Akt S473 phosphorylation is reduced due to a decrease in the amount of SIN1, RICTOR and

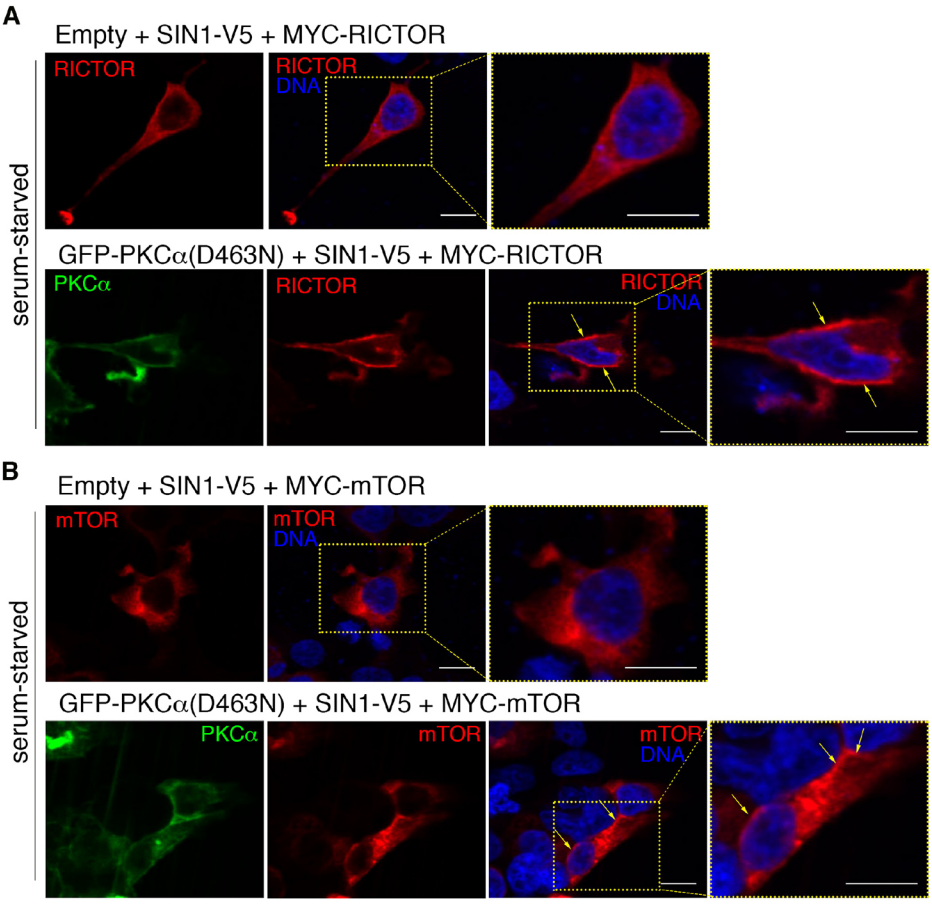

Fig. 8. PKCαD463N expression triggers RICTOR plasma membrane localization. (A) SIN1$^{-/-}$ cells expressing SIN1–V5 and Myc–RICTOR and either empty vector (empty) or GFP–PKCαD463N were serum starved overnight. Cells were then processed in an immunofluorescence assay to detect Myc (RICTOR) and co-stained with DAPI to detect nuclei and imaged through confocal microscopy. (B) SIN1$^{-/-}$ cells expressing SIN1–V5 and Myc–mTOR and either empty vector or GFP–PKCαD463N were serum starved overnight. Cells were then processed in an immunofluorescence assay to detect Myc (mTOR) and co-stained with DAPI to detect nuclei and imaged by confocal microscopy. Yellow arrows indicate plasma membrane localization. Results in A and B show a representative of n=2 biological replicates. Scale bars: 10 µm.

Journal of Cell Science (2019) 132, jcs224931. doi:10.1242/jcs.224931

PKCα in lipid rafts of endothelial cells (Partovian et al., 2008). The authors were able to restore SIN1 and RICTOR levels and Akt S473 phosphorylation by overexpressing a plasma membrane-targeted form of WT PKCα (myristoylated-WT PKCα) in syndecan-4-knockout endothelial cells. Consistent with our results, these authors found that: (1) PKCα can target SIN1 and RICTOR to the plasma membrane, and (2) Akt S473 phosphorylation occurs predominantly at the plasma membrane. However, when this study was published it was unclear how PKCα mediates relocation of SIN1 and RICTOR. From our previous work and others, it is now known that SIN1 interacts directly with PKC and SGK1 through its CRIM domain (Cameron et al., 2011; Lu et al., 2011; Tatebe and Shiozaki, 2017). Thus, we find that SIN1 can recruit mTORC2 and SGK1 to cellular membranes, not only through its PH domain but additionally through its interaction with cPKC. One limitation of our study is the use of SIN1 and SGK1 overexpression since overexpression of these proteins might influence their subcellular localization. However, we see similar results when SIN1 is reconstituted in SIN1$^{-/-}$ cells at levels that reflect endogenous SIN1 expression (see Fig. S8) and with other mTORC2-specific proteins (RICTOR) (Fig. 8A). An interesting direction for future work is understanding how localization of mTORC2 is coordinately regulated by direct binding of lipids to the SIN1 PH domain and indirectly through SIN1 interaction with PKC.

cPKCs interact with cellular membranes through their DAG-binding cysteine-rich zinc finger (C1) domains and Ca^{2+}-dependent phospholipid binding C2 domain (Rosse et al., 2010). cPKC requires three sequential priming phosphorylations that stabilize the protein in an active conformation and, importantly, mask the DAG-binding C1 domains (Rosse et al., 2010). Kinase-dead cPKC mutants do not fold correctly, allowing exposure of the C1 domains and pre-targeting of the kinase to the plasma membrane in the absence of stimulation (Antal et al., 2015). We find that inactivation of cPKC catalytic activity redistributes SIN1 and SGK1 to the plasma membrane in the absence of hormonal stimulation. Aberrant pre-targeting to the plasma membrane likely explains the effect of PKCαD463N expression on the dramatic SIN1 and SGK1 re-localization. Unexpectedly, when SIN1 and SGK1 are pre-targeted by cPKC to the plasma membrane, SGK1 phosphorylation by mTORC2 is prevented. In contrast, Akt S473 phosphorylation is only slightly reduced. Why mTORC2 does not phosphorylate SGK1 when localized in advance at the plasma membrane is a remaining question. One possibility is that catalytically inactive cPKC relocates SIN1, RICTOR and SGK1 to the plasma membrane in the absence of mTOR. Interestingly, Partovian et al. observed that mTOR localization in lipid rafts is not mediated by PKCα suggesting that mTORC2 could form locally at cellular membranes (Partovian et al., 2008). Alternatively, SGK1-associated mTORC2 might require an activating signal that is not present at the plasma membrane. Consistent with this hypothesis, a recent study has shown that plasma membrane-localized mTORC2 is constitutively active whereas endosomal and ER-localized mTORC2 activity requires PI3K activity (Ebner et al., 2017).

Although SGK1 and Akt share considerable similarity within their catalytic domains, their N-terminal domains diverge markedly: Akt isoforms preferentially bind to PIP_3 found at the plasma membrane through their N-terminal pleckstrin homology (PH) domain (Pearce et al., 2010). Akt is also found at the ER, mitochondria and MAMs. However, it is generally thought that T308 phosphorylation by PDK1 occurs at the PM followed by translocation of Akt to internal membranes (Hemmings and Restuccia, 2012). SGK isoforms do not contain a PH domain and instead bind PI(3)P, PI(4)P and PI(5)P through a Phox homology (PX)-like domain in their N-terminus (Pao et al., 2007). A significant consequence of the lack of a PH domain is that, in contrast to Akt, SGK1 requires mTORC2 S422 phosphorylation to create a docking site for PDK1 and the subsequent phosphorylation of its activation loop site residue T256 (Collins et al., 2003). SGK1 has also been found in multiple subcellular compartments including the nucleus (Buse et al., 1999), mitochondria (Engelsberg et al., 2006), endosomes (Engelsberg et al., 2006) and ER (Arteaga et al., 2006; Bogusz et al., 2006; Soundararajan et al., 2005). Consistent with our results, SGK1 has been shown to shuttle between the nucleus, cytoplasm and plasma membrane in response to hormones and other stimuli. Notably, mTORC2 is also reported to shuttle between the nucleus and the cytoplasm in response to rapamycin and the cell cycle (Rosner and Hengstschläger, 2008, 2011). There is evidence that the N-terminal region of SGK1 is responsible for its targeting to cellular membranes, but whether this is through direct binding of SGK1 to phosphoinositides is not clear (Pao et al., 2007). Moreover, it is not known whether SGK1 activation requires localization to a particular membrane domain or organelle. We find that SGK1 localization is influenced by cPKC, presumably through interaction with SIN1. In addition, our findings strongly suggest that, as opposed to Akt, SGK1 is subject to mTORC2 phosphorylation and activation at a perinuclear compartment.

SGK1 is unique among protein kinases in that its activity is regulated at both the transcriptional and enzymatic levels. SGK1 mRNA expression is acutely induced in response to a variety of hormones (Lang et al., 2006). Moreover, SGK1 protein abundance is also regulated post-transcriptionally by rapid ubiquitin-mediated proteolysis involving ER localization and the ER-associated degradation (ERAD) pathway (Arteaga et al., 2006; Brickley et al., 2002; Soundararajan et al., 2005). One explanation for the tight multi-level regulation of SGK1 expression and activation is its key role in the control of blood pressure and K^+ balance through activation of Na^+ reabsorption and K^+ excretion. Our results suggest an intriguing possibility that SGK1 activation occurs in close proximity to its translation, coupling the acute increase in SGK1 protein level with its activation.

In conclusion, our results uncover an important distinction in regulation of the highly related AGC-kinases Akt and SGK1: mTORC2-dependent Akt S473 phosphorylation occurs at the plasma membrane whereas SGK1 S422 phosphorylation occurs at a perinuclear compartment. Moreover, we are able to uncouple activation of Akt and SGK1 by insulin through inhibition of cPKC activity and mis-localization of SGK1 to the plasma membrane. These findings provide new mechanistic insight into how the signaling pathways that control electrolyte balance and metabolic homeostasis are uniquely regulated and will provide a framework for further studies aimed at identifying novel therapies for hypertension-associated metabolic disease.

MATERIALS AND METHODS

Materials

Dulbecco's modified Eagle medium (DMEM), fetal bovine serum (FBS) (JRS), sodium pyruvate and non-essential amino acid supplement were purchased from the UCSF Cell Culture Facility. RIA-grade BSA was purchased from Sigma. L-Glutamine and trypsin were from Corning. G418 was from Gibco. Polyethyleneimine 'MAX' (molecular mass 40,000 Da) transfection reagent was from Polysciences (Cat. #24756). PP242 and PIK90 were kind gifts from Kevan Shokat, UCSF, CA. Gö6986 and Gö6976 were from Calbiochem. CID755653, CRT0066101 and GSK650394 were from Tocris. U0126 was from Cell Signaling Technology. LY333531 was from Enzo Life Sciences. Lambda phosphatase was from New England

Journal of Cell Science (2019) 132, jcs224931. doi:10.1242/jcs.224931

Biolabs (NEB). Losartan, Human Angiotensin II and PMA were from Sigma. Humulin (human insulin) was purchased from the San Francisco General Hospital pharmacy. Bradford Assay Reagent was purchased from ThermoFisher Scientific (Cat. #1856209). 4′,6′-diamidino-2-phenylindole (DAPI) was from ThermoFisher Scientific (Cat #D1306). Fluoromount-G mounting medium was from Southern Biotech (Cat. #0100-01).

Antibodies

Western blotting

Antibodies used for western blotting were against the following: phosphorylated (p)SGK1 S422 (1:1000, sc-16745, Santa Cruz Biotechnology); total SGK1 (1:2000, 5188, Sigma); pAkt S473 (1:1000, 4060, Cell Signaling Technology; CST); total Akt (1:1000, 4691, CST); pERK1/2 T202/Y204 (1:1000, 4370, CST); Total ERK1/2 (1:1000, 4695, CST); pS6K T389 (1:1000, 9234, CST); total S6K (1:1000, 2708, CST); SIN1 (1:1000, 05-1044, Millipore); pSIN1 T86 (1:1000, 14716, CST); V5–HRP (1:2500, MA5-15253, Invitrogen); pPKD S744/S748 (1:1000, 2054, CST); pPKD S916 (1:1000, 2051, CST); Total PKD (1:1000, 90039, CST); pPKC substrate (1:1000, 2261, CST); pPKD substrate (1:1000, 4381, CST); GFP (1:10,000, 8371-2, Clontech); HA–HRP (1:5000, PA1-29751, ThermoFisher Scientific); and tubulin (1:5000, T9026, Sigma).

Immunoprecipitation

Antibodies used for immunoprecipitation were against the following: anti-Flag M2 agarose affinity gel (5-10 µl agarose/1000 µg protein, A2220, Sigma); anti-V5 (~1 µg/1000 µg protein, 37-7500, Invitrogen); and anti-V5 agarose affinity gel (5-10 µl agarose/1000 µg protein, A7345, Sigma).

Immunofluorescence

Antibodies used for immunofluorescence were against the following: SIN1 (1:100, 05-1044, Millipore); SGK1 (1:2000, 5188, Sigma); Alexa-Fluor-647-conjugated donkey anti-rabbit IgG (1:100, A35173, ThermoFisher Scientific); Alexa555-conjugated goat anti-mouse IgG (1:100, A32727, ThermoFisher Scientific); and Myc (1:2000, M4439, Sigma).

Expression constructs

Flag-SGK1, SIN1-V5, and SIN1-Flag in pMO Vector were generated as described previously (Lu et al., 2011). SIN1-V5 (S128A), (S315A), (S356A), (S315A/S356A), (S128A/S315A), (S128A/S315A/S356A) and (S128D/S315D/S356D) were generated using the Quikchange II site-directed mutagenesis kit (Agilent) with pMO-SIN1-V5 as template according to the manufacturer's instructions. AT_1R was purchased from Origene. GFP–PKCα and GFP–PKCα(D463N) were kind gifts from Peter Parker, Francis Crick Institute, London, UK. HA–PKD1 and HA-PKD(S738E/S742E) were Addgene plasmids #10808 and #10810 (deposited by Alex Toker). Myc–RICTOR and Myc–mTOR were Addgene plasmids #1860 and #1861 (deposited by David Sabatini) (Sancak et al., 2010; Sancak et al., 2008; Sarbassov et al., 2004).

Generation of SIN1-knockout HEK293T cells by CRISPR/Cas9

A single guide (sg)RNA with the sequence, 5′-GTATTCCAAATTT-GATGGCA-3′, was designed for targeting the 3′ end of exon 3 of the human *MAPKAP1* genomic locus. The sgRNA sequence driven by a U6 promoter was cloned into the plentiCRISPR V2 vector (Addgene plasmid #52961; deposited by Feng Zhang) that also expresses Cas9 using standard subcloning techniques. The lentiviral plasmid DNA was then packaged into lentivirus by co-transfection with Virapower (Invitrogen) in HEK293FT cells. Supernatant containing lentivirus was used to infect HEK293T cells and then infected cells were selected in puromycin (3 µg/ml). Single colonies were selected by fluorescence-activated cell sorting (FACS) into a 96-well plate, and expanded and tested for SIN1 expression by western blotting.

Cell culture, transfection and treatment

HEK293T, HEK293-AT_1R, and HEK293T-$SIN1^{-/-}$ cells were maintained in DMEM with 2 mM L-glutamine and 10% FBS. HEK293-AT_1R cells (a kind gift from Tamas Balla, Intramural Research Program, NIH NICHD, Baltimore, MD) stably express double HA- and Flag-tagged AT_1R. HEK293FT cells (ATCC) were used to produce high-titer lentiviral particles and were maintained in DMEM with sodium pyruvate, non-essential amino acids, 2 mM L-glutamine, 500 µg/ml G418 and 10% FBS. The opossum kidney proximal tubule cell line (OKP) (a kind gift from Orson Moe, UTSW, Dallas, TX) was maintained in DMEM with 2 mM glutamine and 10% FBS. These cell lines were routinely tested for mycoplasma contamination. All cell lines were acquired from reputable sources but have not recently been authenticated. All cell lines were transfected using polyethyleneimine 'MAX' (molecular mass 40,000 Da). For all experiments, cells were serum-starved in DMEM containing 0.1% BSA overnight. For inhibitor assays, cells were treated for 15–30 min with 10 µM losartan, 300 nM PP242, 25 nM rapamycin, 5 µM Gö6976, 5 µM Gö6983, 25 µM CID655763, 5 µM CRT0066101, 200 nM LY333531, 1 µM PIK90, 10 µM U0126 or vehicle (DMSO), followed by 200 nM angiotensin II (AngII) or 200 nM insulin as indicated in figure legends.

Immunoprecipitation and western blotting

Cells were rinsed once with ice-cold PBS, lysed in 1% Triton X-100 buffer (40 mM HEPES pH 7.5, 1 mM EDTA pH 8, 10 mM sodium pyrophosphate, 10 mM glycerophosphate, 50 mM sodium fluoride, 120 mM sodium chloride and 1% Triton X-100), and centrifuged at 10,000 r.p.m. for 10 min. Supernatant (cell extract) was removed and protein content estimated by performing a Bradford assay. Cell extract (15–40 µg protein) was separated by SDS-PAGE and transferred to PVDF membranes. To immunoprecipitate Flag–SGK1, 0.1–1 mg of cell extract protein was rotated overnight at 4°C with 10–20 µl 50% slurry anti-FLAG affinity gel. The agarose beads were collected by centrifugation, washed three times with 1% Triton X-100 cell lysis buffer, boiled and denatured in 1× Laemmli sample buffer, separated by SDS-PAGE and transferred to PVDF membrane. To immunoprecipitate SIN1–V5, 50–200 µg of cell extract protein was rotated overnight at 4°C with ~1 µg anti-V5 antibody or 10–20 µl 50% slurry anti-V5-affinity gel. For immunoprecipitations with unconjugated antibody, 10 µl 50% slurry protein A/G-conjugated agarose beads (Santa Cruz Biotechnology) was added and lysates were rotated at 4°C for an additional hour. The agarose beads were collected by centrifugation (8,000 r.p.m. for 30 s), washed three times with cell lysis buffer, boiled and denatured in 1× Laemmli sample buffer, separated by SDS-PAGE and transferred to PVDF. Membranes were blocked in TBS plus 0.1% Tween-20 (TBS-T) containing 5% skim milk and incubated with the relevant primary antibodies for either 1–2 h at room-temperature (total SGK1, pAkt S473, tubulin, GFP, V5, and HA) or overnight at 4°C in blocking buffer containing 5% BSA (phospho-antibodies) or 5% milk (all other antibodies). After incubation with primary antibodies, membranes were washed in TBS-T and then incubated with HRP-labeled secondary antibodies for 1 h. Membranes were washed again in TBS-T, incubated with ECL reagent (GE Healthcare) and exposed to film. Quantification of western blots was performed on scanned films with NIH ImageJ Software.

Confocal imaging and analysis

Cells were fixed with 3.7% formaldehyde in modified Brinkley Buffer 1980 (80 mM PIPES pH 6.8, 1 mM $CaCl_2$ and 1 mM $MgCl_2$) for 20 min at room temperature. The fixation solution was removed by washing in PBS. The fixed cells were permeabilized and blocked by incubation in TBS containing 3% BSA and 0.1% Triton X-100 for 20 min. Primary antibodies were diluted in TBS containing 3% BSA and 0.1% Triton X-100. Cells were co-stained with DAPI to identify nuclei. Coverslips were mounted on slides in Fluoromount-G. *Z*-stack images were collected on a Yokagawa CSU22 spinning disk confocal microscope with a 40×, 0.95 NA, plan APO dry objective. These are all adjectives describing the objective. The middle slice of the *z*-stack was used for all representative images. Quantification of images was performed on average intensity *z* projections using ImageJ software (http://rsb.info.nih.gov/ij). For each image, the percentage of nuclear-localized SIN1 and SGK1 was calculated by first selecting the nuclear region of interests (ROIs) in the DAPI channel and measuring fluorescence intensity within those ROIs in either the SIN1 (Alexa Fluor 555) or SGK1 (Alexa Fluor 647) channels. Then, ROIs were created for total SIN1 or SGK1 and fluorescence intensity was measured in the appropriate channel. The percentage nuclear localization was determined by dividing nuclear fluorescence intensity by total SIN1 or SGK1 fluorescence intensity. Analysis of SIN1 and SGK1 intensity profiles was carried out using the ImageJ Plot Profile function.

Mass spectrometry

HEK-293T cells were transiently transfected with pMO empty vector, SIN1-flag and WT GFP–PKCα or SIN1–Flag and GFP PKCα(D463N). After overnight serum starvation, cells were stimulated with 1 µM PMA for 15 min. Cells were lysed and SIN1 immunoprecipitated from 5 mg protein extract by overnight incubation with anti-Flag Affinity agarose. In separate experiments, HEK-293-AT_1R cells were transiently transfected with empty pMO vector or SIN1–Flag. After overnight serum starvation, cells were stimulated with 200 nM Ang II either in combination with vehicle (DMSO), 5 µM Gö6983 or 5 µM Gö6976. Cells were lysed and SIN1 immunoprecipitated from 5 mg protein extract by overnight incubation with anti-Flag-conjugated agarose beads (Sigma). Immunoprecipitated SIN1 was separated on SDS-PAGE and visualized by staining with Coomassie Blue (BioRad).

Gel pieces containing SIN1–flag were excised and digested in-gel as described previously (Rosenfeld et al., 1992). The extracted digests were vacuum-evaporated and resuspended in 10 µl 0.1% formic acid in water, and analyzed by nanoflow ultra-performance liquid chromatography tandem mass spectrometry (UPLC-MS/MS). Peptides were separated by nano-flow liquid chromatography using a 75-µm×150-mm reverse phase C18 column PepMap® C18 EasySpray column (ThermoFisher Scientific) packed with 3 µm particles, at a flow rate of 300 nl/min in a NanoAcquity UPLC system (Waters). Mobile phase A was 0.1% formic acid in water, and mobile phase B was 0.1% formic acid in acetonitrile. Following equilibration of the column in 2% solvent B, an aliquot of each digest (5 µl) was injected, then the organic content of the mobile phase was increased linearly to 30% over 60 min, and then to 50% in 2 min. The liquid chromatography eluate was coupled to a hybrid linear ion trap-Orbitrap mass spectrometer (LTQ-Orbitrap Velos, ThermoFisher Scientific). Peptides were analyzed in positive ion mode and in information-dependent acquisition mode to automatically switch between MS and MS/MS acquisition. MS spectra were acquired in profile mode using the Orbitrap analyzer in the m/z range between 350 and 1500. For each MS spectrum, the six most-intense multiple charged ions over a threshold of 1000 counts were selected to perform collision-induced dissociation experiments. Product ions were analyzed in the linear ion trap in centroid mode. A dynamic exclusion window of 0.5 Da was applied that prevented the same m/z from being selected for 60 s after its acquisition.

Peak lists were generated using PAVA in-house software (Guan et al., 2011), based on the RawExtract script from Xcalibur v2.4 (ThermoFisher Scientific). The peak lists were searched against the human and murine subset of the SwissProt database of March 21 2012, containing 36775 entries, using in-house ProteinProspector version 5.10.17 (a public version is available on line) (Clauser et al., 1999). A randomized version of all entries was concatenated to the database for estimation of false discovery rates in the searches. Peptide tolerance in searches was 20 ppm for precursor and 0.6 Da for product ions, respectively. Enzyme specificity was set to trypsin or GluC as appropriate. Peptides containing two miscleavages were allowed. Carboxymethylation of cysteine was allowed as constant modification; acetylation of the N terminus of the protein, pyroglutamate formation from N terminal glutamine, oxidation of methionine, and phosphorylation of serine, theonine and tyrosine were allowed as variable modifications. The number of modifications was limited to two per peptide. A minimal ProteinProspector protein score of 20, a peptide score of 15, a maximum expectation value of 0.004 for protein and 0.02 for peptides (for tryptic searches), or 0.001 for protein and 0.005 for peptides (for GluC searches), and a minimal discriminant score threshold of 0.0 were used for identification criteria. The false discovery rate (FDR) was below 1%.in all cases

For relative quantitation of the phosphopeptide abundances between samples, the total intensity for precursor ions on the MS traces was integrated during the elution time using the Xcalibur Qual browser (ThermoFisher Scientific) or Skyline (Schilling et al., 2012). Levels were normalized between samples using non-phosphorylated peptides of SIN1, and expressed as ratios to the un-stimulated sample.

Statistics

Statistical analysis was performed in Microsoft Excel using the Analysis Toolpak Add-In. Sample sizes (biological replicates) are listed in the figure legends. One-way ANOVA was used to determine differences between groups followed by unpaired two-tailed t-tests.

Acknowledgements

We thank David Bryant (Beatson Institute, Glasgow, Scotland, UK) for reagents and for critical review of the manuscript. We also thank Kaveh Ashrafi (UCSF, San Francisco, CA) for critical review of the manuscript. We thank Brad Heller for reagents and methods used in generation of CRISPR-mediated HEK-293T$^{SIN1-/-}$ cells. We also thank Roshanak Irannejad and Jacob Bendor for methods and helpful discussions regarding immunostaining and quantification of confocal images.

Competing interests

The authors declare no competing or financial interests.

Author contributions

Conceptualization: C.E.G., D.P.; Methodology: C.E.G., J.A.O.-P., K.H.L.; Validation: C.E.G.; Formal analysis: C.E.G., J.A.O.-P.; Investigation: C.E.G., K.H.L., B.S., G.S.; Resources: C.E.G., A.L.B., D.P.; Data curation: J.A.O.-P.; Writing - original draft: C.E.G., D.P.; Writing - review & editing: C.E.G., J.A.O.-P., A.L.B., D.P.; Visualization: C.E.G.; Supervision: C.E.G., D.P.; Funding acquisition: C.E.G., A.L.B., D.P.

Funding

This work was supported by National Institutes of Health (NIH) grants from the National Institute of Diabetic, Digestive and Kidney Diseases (DK56695 to D.P.; T32 DK007219 and K01 DK983313 to C.E.G.) as well as by the James Hilton Manning and Emma Austin Manning Foundation (to D.P.). Mass spectrometry experiments were performed at the Biomedical Mass Spectrometry Resource at UCSF (A.L.B., Director) supported by funding from the Biomedical Technology Research Centers Program of the NIH National Institute of General Medical Sciences, NIH NIGMS 8P41GM103481 and Howard Hughes Medical Institute. Deposited in PMC for release after 12 months.

Supplementary information

Supplementary information available online at
http://jcs.biologists.org/lookup/doi/10.1242/jcs.224931.supplemental

References

Alessi, D. R., Pearce, L. R. and Garcia-Martinez, J. M. (2009). New insights into mTOR signaling: mTORC2 and beyond. *Sci. Signal.* **2**, pe27.

Antal, C. E., Violin, J. D., Kunkel, M. T., Skovso, S. and Newton, A. C. (2014). Intramolecular conformational changes optimize protein kinase C signaling. *Chem. Biol.* **21**, 459-469.

Antal, C. E., Callender, J. A., Kornev, A. P., Taylor, S. S. and Newton, A. C. (2015). Intramolecular C2 domain-mediated autoinhibition of protein kinase C betaII. *Cell Rep.* **12**, 1252-1260.

Arteaga, M. F., Wang, L., Ravid, T., Hochstrasser, M. and Canessa, C. M. (2006). An amphipathic helix targets serum and glucocorticoid-induced kinase 1 to the endoplasmic reticulum-associated ubiquitin-conjugation machinery. *Proc. Natl. Acad. Sci. USA* **103**, 11178-11183.

Baskin, R. and Sayeski, P. P. (2012). Angiotensin II mediates cell survival through upregulation and activation of the serum and glucocorticoid inducible kinase 1. *Cell. Signal.* **24**, 435-442.

Betz, C. and Hall, M. N. (2013). Where is mTOR and what is it doing there? *J. Cell Biol.* **203**, 563-574.

Bogusz, A. M., Brickley, D. R., Pew, T. and Conzen, S. D. (2006). A novel N-terminal hydrophobic motif mediates constitutive degradation of serum- and glucocorticoid-induced kinase-1 by the ubiquitin-proteasome pathway. *FEBS J.* **273**, 2913-2928.

Brickley, D. R., Mikosz, C. A., Hagan, C. R. and Conzen, S. D. (2002). Ubiquitin modification of serum and glucocorticoid-induced protein kinase-1 (SGK-1). *J. Biol. Chem.* **277**, 43064-43070.

Brunet, A., Park, J., Tran, H., Hu, L. S., Hemmings, B. A. and Greenberg, M. E. (2001). Protein kinase SGK mediates survival signals by phosphorylating the forkhead transcription factor FKHRL1 (FOXO3a). *Mol. Cell. Biol.* **21**, 952-965.

Buse, P., Tran, S. H., Luther, E., Phu, P. T., Aponte, G. W. and Firestone, G. L. (1999). Cell cycle and hormonal control of nuclear-cytoplasmic localization of the serum- and glucocorticoid-inducible protein kinase, Sgk, in mammary tumor cells. A novel convergence point of anti-proliferative and proliferative cell signaling pathways. *J. Biol. Chem.* **274**, 7253-7263.

Cameron, A. J. M., Linch, M. D., Saurin, A. T., Escribano, C. and Parker, P. J. (2011). mTORC2 targets AGC kinases through Sin1-dependent recruitment. *Biochem. J.* **439**, 287-297.

Carey, R. M. (2011). Overview of endocrine systems in primary hypertension. *Endocrinol. Metab. Clin. North Am.* **40**, 265-277, vii.

Clauser, K. R., Baker, P. and Burlingame, A. L. (1999). Role of accurate mass measurement (±10 ppm) in protein identification strategies employing MS or MS/MS and database searching. *Anal. Chem.* **71**, 2871-2882.

Collins, B. J., Deak, M., Arthur, J. S., Armit, L. J. and Alessi, D. R. (2003). In vivo role of the PIF-binding docking site of PDK1 defined by knock-in mutation. *EMBO J.* **22**, 4202-4211.
Daub, H., Weiss, F. U., Wallasch, C. and Ullrich, A. (1996). Role of transactivation of the EGF receptor in signalling by G-protein-coupled receptors. *Nature* **379**, 557-560.
Dibble, C. C., Asara, J. M. and Manning, B. D. (2009). Characterization of Rictor phosphorylation sites reveals direct regulation of mTOR complex 2 by S6K1. *Mol. Cell. Biol.* **29**, 5657-5670.
Ebner, M., Sinkovics, B., Szczygiel, M., Ribeiro, D. W. and Yudushkin, I. (2017). Localization of mTORC2 activity inside cells. *J. Cell Biol.* **216**, 343-353.
Engelsberg, A., Kobelt, F. and Kuhl, D. (2006). The N-terminus of the serum- and glucocorticoid-inducible kinase Sgk1 specifies mitochondrial localization and rapid turnover. *Biochem. J.* **399**, 69-76.
Gan, X., Wang, J., Su, B. and Wu, D. (2011). Evidence for direct activation of mTORC2 kinase activity by phosphatidylinositol 3,4,5-trisphosphate. *J. Biol. Chem.* **286**, 10998-11002.
Gaubitz, C., Prouteau, M., Kusmider, B. and Loewith, R. (2016). TORC2 Structure and Function. *Trends Biochem. Sci.* **41**, 532-545.
Guan, S., Price, J. C., Prusiner, S. B., Ghaemmaghami, S. and Burlingame, A. L. (2011). A data processing pipeline for mammalian proteome dynamics studies using stable isotope metabolic labeling. *Mol. Cell. Proteomics* **10**, M111 010728.
Hein, L., Meinel, L., Pratt, R. E., Dzau, V. J. and Kobilka, B. K. (1997). Intracellular trafficking of angiotensin II and its AT1 and AT2 receptors: evidence for selective sorting of receptor and ligand. *Mol. Endocrinol.* **11**, 1266-1277.
Hemmings, B. A. and Restuccia, D. F. (2012). PI3K-PKB/Akt pathway. *Cold Spring Harb. Perspect. Biol.* **4**, a011189.
Herrera, M. and Coffman, T. M. (2012). The kidney and hypertension: novel insights from transgenic models. *Curr. Opin Nephrol. Hypertens.* **21**, 171-178.
Higuchi, S., Ohtsu, H., Suzuki, H., Shirai, H., Frank, G. D. and Eguchi, S. (2007). Angiotensin II signal transduction through the AT1 receptor: novel insights into mechanisms and pathophysiology. *Clin. Sci. (Lond.)* **112**, 417-428.
Humphrey, S. J., Yang, G., Yang, P., Fazakerley, D. J., Stöckli, J., Yang, J. Y. and James, D. E. (2013). Dynamic adipocyte phosphoproteome reveals that Akt directly regulates mTORC2. *Cell Metab.* **17**, 1009-1020.
Hunyady, L. and Catt, K. J. (2006). Pleiotropic AT1 receptor signaling pathways mediating physiological and pathogenic actions of angiotensin II. *Mol. Endocrinol.* **20**, 953-970.
Hunyady, L., Baukal, A. J., Gáborik, Z., Olivares-Reyes, J. A., Bor, M., Szaszák, M., Lodge, R., Catt, K. J. and Balla, T. (2002). Differential PI 3-kinase dependence of early and late phases of recycling of the internalized AT1 angiotensin receptor. *J. Cell Biol.* **157**, 1211-1222.
Irannejad, R., Tsvetanova, N. G., Lobingier, B. T. and VON Zastrow, M. (2015). Effects of endocytosis on receptor-mediated signaling. *Curr. Opin. Cell Biol.* **35**, 137-143.
Kennedy, B. K. and Lamming, D. W. (2016). The mechanistic target of rapamycin: the grand ConducTOR of metabolism and aging. *Cell Metab.* **23**, 990-1003.
Lang, F., Böhmer, C., Palmada, M., Seebohm, G., Strutz-Seebohm, N. and Vallon, V. (2006). (Patho)physiological significance of the serum- and glucocorticoid-inducible kinase isoforms. *Physiol. Rev.* **86**, 1151-1178.
Liu, P., Gan, W., Inuzuka, H., Lazorchak, A. S., Gao, D., Arojo, O., Liu, D., Wan, L., Zhai, B., Yu, Y. et al. (2013). Sin1 phosphorylation impairs mTORC2 complex integrity and inhibits downstream Akt signalling to suppress tumorigenesis. *Nat. Cell Biol.* **15**, 1340-1350.
Liu, P., Gan, W., Chin, Y. R., Ogura, K., Guo, J., Zhang, J., Wang, B., Blenis, J., Cantley, L. C., Toker, A. et al. (2015a). PtdIns(3,4,5)P3-dependent activation of the mTORC2 kinase complex. *Cancer Discov.* **5**, 1194-1209.
Liu, P., Gan, W., Guo, C., Xie, A., Gao, D., Guo, J., Zhang, J., Willis, N., Su, A., Asara, J. M. et al. (2015b). Akt-mediated phosphorylation of XLF impairs non-homologous end-joining DNA repair. *Mol. Cell* **57**, 648-661.
Lu, D., Yang, H., Shaw, G. and Raizada, M. K. (1998). Angiotensin II-induced nuclear targeting of the angiotensin type 1 (AT1) receptor in brain neurons. *Endocrinology* **139**, 365-375.
Lu, M., Wang, J., Ives, H. E. and Pearce, D. (2011). mSIN1 protein mediates SGK1 protein interaction with mTORC2 protein complex and is required for selective activation of the epithelial sodium channel. *J. Biol. Chem.* **286**, 30647-30654.
Moe, O. W., Miller, R. T., Horie, S., Cano, A., Preisig, P. A. and Alpern, R. J. (1991). Differential regulation of Na/H antiporter by acid in renal epithelial cells and fibroblasts. *J. Clin. Invest.* **88**, 1703-1708.
Pao, A. C., Mccormick, J. A., Li, H., Siu, J., Govaerts, C., Bhalla, V., Soundararajan, R. and Pearce, D. (2007). NH2 terminus of serum and glucocorticoid-regulated kinase 1 binds to phosphoinositides and is essential for isoform-specific physiological functions. *Am. J. Physiol. Renal. Physiol.* **292**, F1741-F1750.
Park, J., Leong, M. L., Buse, P., Maiyar, A. C., Firestone, G. L. and Hemmings, B. A. (1999). Serum and glucocorticoid-inducible kinase (SGK) is a target of the PI 3-kinase-stimulated signaling pathway. *EMBO J.* **18**, 3024-3033.
Partovian, C., Ju, R., Zhuang, Z. W., Martin, K. A. and Simons, M. (2008). Syndecan-4 regulates subcellular localization of mTOR Complex2 and Akt activation in a PKCalpha-dependent manner in endothelial cells. *Mol. Cell* **32**, 140-149.
Pearce, L. R., Komander, D. and Alessi, D. R. (2010). The nuts and bolts of AGC protein kinases. *Nat. Rev. Mol. Cell Biol.* **11**, 9-22.
Rosenfeld, J., Capdevielle, J., Guillemot, J. C. and Ferrara, P. (1992). In-gel digestion of proteins for internal sequence analysis after one- or two-dimensional gel electrophoresis. *Anal. Biochem.* **203**, 173-179.
Rosner, M. and Hengstschläger, M. (2008). Cytoplasmic and nuclear distribution of the protein complexes mTORC1 and mTORC2: rapamycin triggers dephosphorylation and delocalization of the mTORC2 components rictor and sin1. *Hum. Mol. Genet.* **17**, 2934-2948.
Rosner, M. and Hengstschläger, M. (2011). mTOR protein localization is cell cycle-regulated. *Cell Cycle* **10**, 3608-3610.
Rosse, C., Linch, M., Kermorgant, S., Cameron, A. J. M., Boeckeler, K. and Parker, P. J. (2010). PKC and the control of localized signal dynamics. *Nat. Rev. Mol. Cell Biol.* **11**, 103-112.
Rozengurt, E. (2007). Mitogenic signaling pathways induced by G protein-coupled receptors. *J. Cell. Physiol.* **213**, 589-602.
Saci, A., Cantley, L. C. and Carpenter, C. L. (2011). Rac1 regulates the activity of mTORC1 and mTORC2 and controls cellular size. *Mol. Cell* **42**, 50-61.
Sancak, Y., Peterson, T. R., Shaul, Y. D., Lindquist, R. A., Thoreen, C. C., Bar-Peled, L. and Sabatini, D. M. (2008). The Rag GTPases bind raptor and mediate amino acid signaling to mTORC1. *Science* **320**, 1496-1501.
Sancak, Y., Bar-Peled, L., Zoncu, R., Markhard, A. L., Nada, S. and Sabatini, D. M. (2010). Ragulator-Rag complex targets mTORC1 to the lysosomal surface and is necessary for its activation by amino acids. *Cell* **141**, 290-303.
Sarbassov, D. D., Ali, S. M., Kim, D.-H., Guertin, D. A., Latek, R. R., Erdjument-Bromage, H., Tempst, P. and Sabatini, D. M. (2004). Rictor, a novel binding partner of mtor, defines a rapamycin-insensitive and raptor-independent pathway that regulates the cytoskeleton. *Curr. Biol.* **14**, 1296-1302.
Schilling, B., Rardin, M. J., Maclean, B. X., Zawadzka, A. M., Frewen, B. E., Cusack, M. P., Sorensen, D. J., Bereman, M. S., Jing, E., Wu, C. C. et al. (2012). Platform-independent and label-free quantitation of proteomic data using MS1 extracted ion chromatograms in skyline: application to protein acetylation and phosphorylation. *Mol. Cell. Proteomics* **11**, 202-214.
Shah, B. H., Yesilkaya, A., Olivares-Reyes, J. A., Chen, H.-D., Hunyady, L. and Catt, K. J. (2004). Differential pathways of angiotensin II-induced extracellularly regulated kinase 1/2 phosphorylation in specific cell types: role of heparin-binding epidermal growth factor. *Mol. Endocrinol.* **18**, 2035-2048.
Soundararajan, R., Zhang, T. T., Wang, J., Vandewalle, A. and Pearce, D. (2005). A novel role for glucocorticoid-induced leucine zipper protein in epithelial sodium channel-mediated sodium transport. *J. Biol. Chem.* **280**, 39970-39981.
Steinberg, S. F. (2012). Regulation of protein kinase D1 activity. *Mol. Pharmacol.* **81**, 284-291.
Stevens, V. A., Saad, S., Poronnik, P., Fenton-Lee, C. A., Polhill, T. S. and Pollock, C. A. (2008). The role of SGK-1 in angiotensin II-mediated sodium reabsorption in human proximal tubular cells. *Nephrol. Dial. Transplant.* **23**, 1834-1843.
Tatebe, H. and Shiozaki, K. (2017). Evolutionary conservation of the components in the TOR signaling pathways. *Biomolecules* **7**, E77.
Tatebe, H., Murayama, S., Yonekura, T., Hatano, T., Richter, D., Furuya, T., Kataoka, S., Furuita, K., Kojima, C. and Shiozaki, K. (2017). Substrate specificity of TOR complex 2 is determined by a ubiquitin-fold domain of the Sin1 subunit. *eLife* **6**, e19594.
Toker, A. and Marmiroli, S. (2014). Signaling specificity in the Akt pathway in biology and disease. *Adv. Biol. Regul.* **55**, 28-38.
Treins, C., Warne, P. H., Magnuson, M. A., Pende, M. and Downward, J. (2010). Rictor is a novel target of p70 S6 kinase-1. *Oncogene* **29**, 1003-1016.
Yang, G., Murashige, D. S., Humphrey, S. J. and James, D. E. (2015). A positive feedback loop between Akt and mTORC2 via SIN1 phosphorylation. *Cell Rep.* **12**, 937-943.
Zinzalla, V., Stracka, D., Oppliger, W. and Hall, M. N. (2011). Activation of mTORC2 by association with the ribosome. *Cell* **144**, 757-768.

SUPPLEMENTARY INFORMATION

Phosphorylation at distinct subcellular locations underlies specificity in mTORC2 activation of SGK1 and Akt

Catherine E. Gleason[1*], Juan A. Oses-Prieto[2], Kathy H. Li[2], Bidisha Saha[1], Gavin Situ[1], Alma L. Burlingame[2] and David Pearce[1]

[1]Department of Medicine, Division of Nephrology, UCSF, San Francisco, California, USA, 94143; and [2]Departments of Chemistry and Pharmaceutical Chemistry, UCSF, San Francisco, CA, USA, 94143

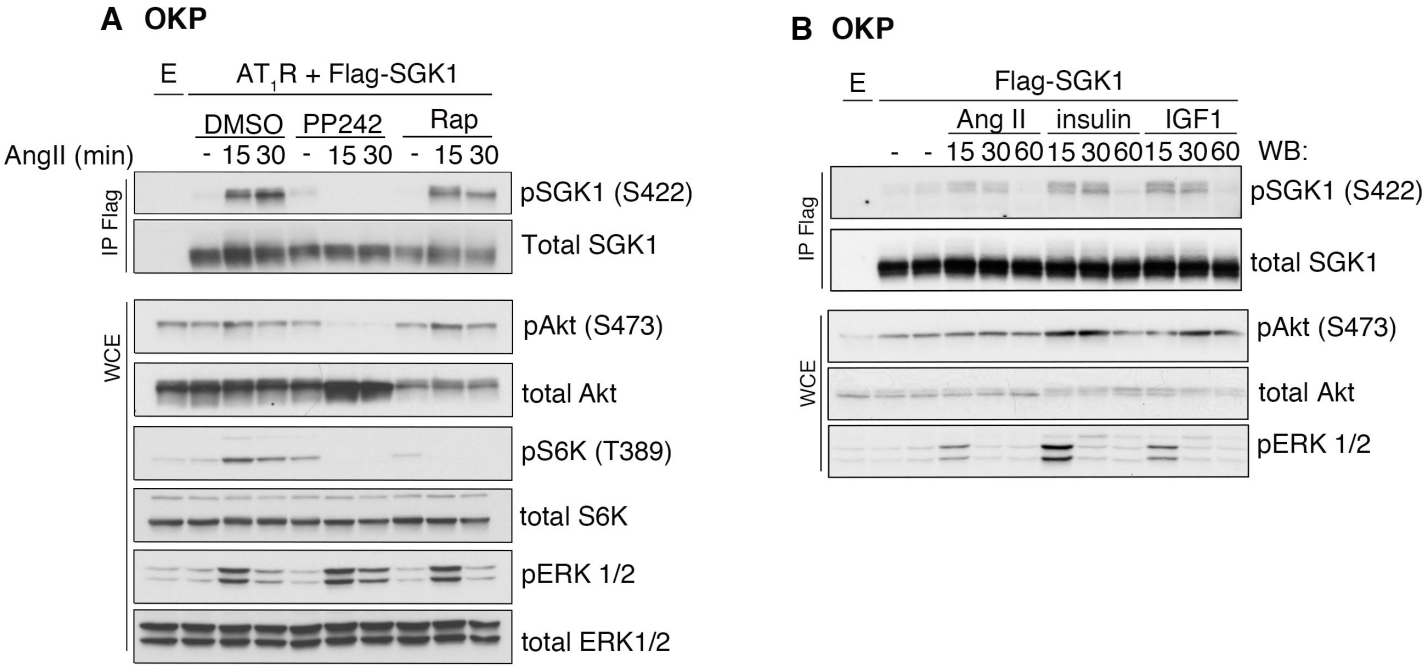

Figure S1, related to Figure 1. AngII stimulates mTORC2-dependent SGK1 S422 phosphorylation in OKP proximal tubule cells.
(A) Western blot of immunoprecipitates and WCE derived from AT1R and Flag-SGK1-transfected OKP cells, serum-starved overnight and then stimulated with 200 nM AngII for the indicated times. E, empty vector.
(B) Western blot of immunoprecipitates and WCE derived from Flag-SGK1 transfected OKP cells, serum-starved overnight and then stimulated with either 400 nM AngII, 200 nM insulin or 50 ng/ml IGF1 for the indicated times. E, empty vector.
(A and B, 3 biological replicates)

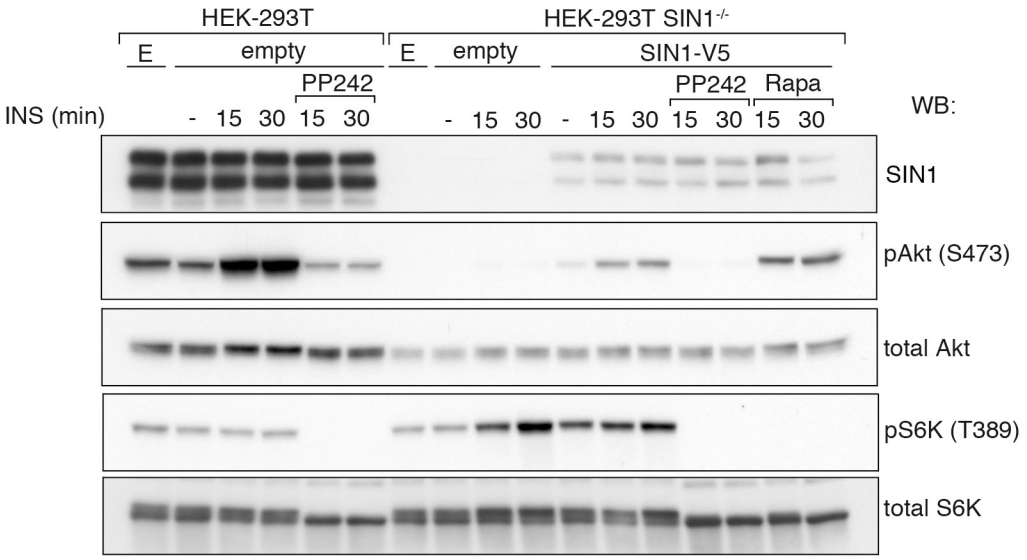

Figure S2, related to Figure 1. Characterization of HEK-293T SIN1$^{-/-}$ cells. Western blot analysis of WCE derived from either HEK-293T cells transfected with empty vector or HEK-293T SIN1$^{-/-}$ cells transfected with empty vector or WT SIN1-V5 as indicated (E, empty vector). Cells were serum-starved overnight before treatment with 200 nM insulin. Where indicated,300 nM PP242 or 25 nM rapamycin were added. (n=3 biological replicates).

A. Tryptic digests (83.7% coverage)

1 **Acc. #:** Q8BKH7 **Uniprot ID:** SIN1_MOUSE **Species:** MOUSE **Name:** Target of Rapamycin Complex 2 subunit MAPKAP1
Organism: Mus musculus **Gene:** Mapkap1 **Existence:** Evidence at protein level **Version:** 1
Protein MW: 59009.2 **Protein pI:** 7.2 **Protein Length:** 522 **Index:** 416897

```
1   MAFLDNPTII LAHIRQSHVT SDDTGMCEMV LIDHDVDLEK THPPSVPGDS GSEVQGSSGE TQGYIYAQSV DITSSWDFGI
81  RRRSNTAQRL ERLRKERQNQ IKCKNIQWKE RNSKQSAQEL KSLFEKKSLK EKPPSSGKQS ILSVRLEQCP LQLNNPFNEY
161 SKFDGKGHVG TTATKKIDVY LPLHSSQDRL LPMTVVTMAS ARVQDLIGLI CWQYTSEGRE PKLNDNVSAY CLHIAEDDGE
241 VDTDFPPLDS NEPIHKFGFS TLALVEKYSS PGLTSKESLF VRINAAHGFS LIQVDNTKVT MKEILLKAVK RRKGSQKISG
321 PQYRLEKQSE PNIAVDLEST LESQNAWEFC LVRENSSRAD GVFEEDSQID IATVQDMLSS HHYKSFKVSM IHRLRFTTDV
401 QLGISGDKVE IDPVTNQKAS TKFWIKQKPI SIDCDLLCAC DLAEEKSPSH AVFKLTYLSS HDYKHLYFES DAATVSEIVL
481 KVNYILESRA STARADYLAQ KQRKLNRRTS FSFQKEKKSG QQ
```

B. GluC digests (63.2% coverage).

Acc. #: Q8BKH7 **Uniprot ID:** SIN1_MOUSE **Species:** MOUSE **Name:** Target of Rapamycin Complex 2 subunit MAPKAP1
Organism: Mus musculus **Gene:** Mapkap1 **Existence:** Evidence at protein level **Version:** 1
Protein MW: 59009.2 **Protein pI:** 7.2 **Protein Length:** 522 **Index:** 416897

```
1   MAFLDNPTII LAHIRQSHVT SDDTGMCEMV LIDHDVDLEK THPPSVPGDS GSEVQGSSGE TQGYIYAQSV DITSSWDFGI
81  RRRSNTAQRL ERLRKERQNQ IKCKNIQWKE RNSKQSAQEL KSLFEKKSLK EKPPSSGKQS ILSVRLEQCP LQLNNPFNEY
161 SKFDGKGHVG TTATKKIDVY LPLHSSQDRL LPMTVVTMAS ARVQDLIGLI CWQYTSEGRE PKLNDNVSAY CLHIAEDDGE
241 VDTDFPPLDS NEPIHKFGFS TLALVEKYSS PGLTSKESLF VRINAAHGFS LIQVDNTKVT MKEILLKAVK RRKGSQKISG
321 PQYRLEKQSE PNIAVDLEST LESQNAWEFC LVRENSSRAD GVFEEDSQID IATVQDMLSS HHYKSFKVSM IHRLRFTTDV
401 QLGISGDKVE IDPVTNQKAS TKFWIKQKPI SIDCDLLCAC DLAEEKSPSH AVFKLTYLSS HDYKHLYFES DAATVSEIVL
481 KVNYILESRA STARADYLAQ KQRKLNRRTS FSFQKEKKSG QQ
```

Figure S3, related to Figure 5. Sequence coverage maps of the MS analysis of SIN1. A) Tryptic digestion; B) GluC digestion. Peptides identified in the MS analysis of the enzymatic digestions are shown in red. Unambiguous phosphorylation sites are highlighted in dark blue. Ambiguous assignments are shown in green.

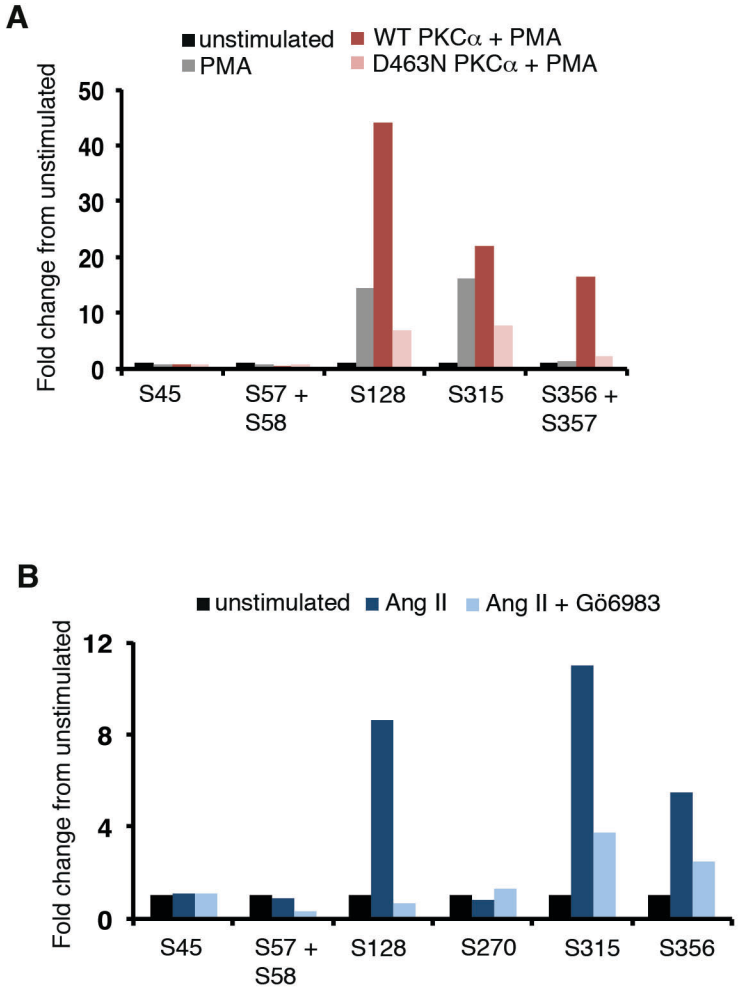

Figure S4, related to Figure 5. Identification of SIN1 phosphorylation sites by LC-MS/MS phospho-site mapping.

(A) Relative quantification of phosphopeptide abundance. HEK-293 cells were transfected with empty vector, SIN1-Flag, and either WT PKCα or PKCαD463N. Cells were left unstimulated or stimulated with 1 mM PMA as indicated for 15 min.

(B), HEK-293-AT_1R cells were transfected with empty vector or SIN1-Flag followed by stimulation with 200 nM Ang II either in the presence of DMSO (vehicle) or the PKC inhibitor, Gö6983 (5 mM) for 60 min.

Both A and B show MS results for GluC SIN1-flag digestion. Graphs depict fold change in phosphopeptide abundance from the unstimulated condition for one representative experiment. (A and B, 3 biological replicates)

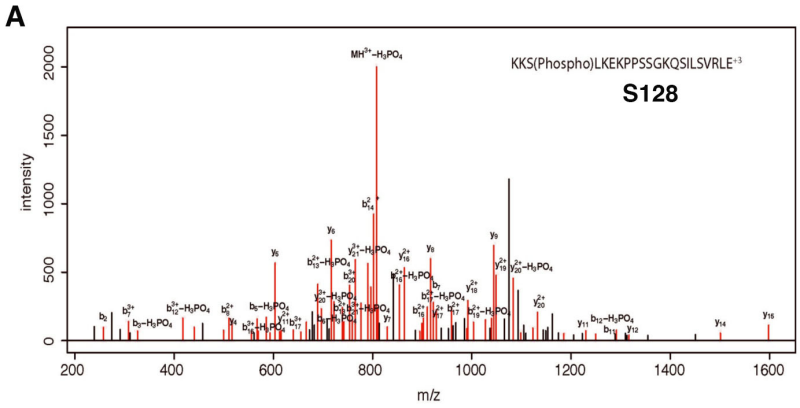

Main Sequence Ions

b-H_3PO_4	b-$H_3PO_4^{+2}$	b	b^{+2}				y	y^{+2}	y-H_3PO_4	y-$H_3PO_4^{+2}$
---	---	---	---	1	K	22	---	---	---	---
---	---	257.1972	*129.1022*	2	K	21	*2391.3007*	1196.1540	*2293.3238*	1147.1655
326.2187	*163.6130*	424.1956	*212.6014*	3	S(Phospho)	20	*2263.2057*	1132.1065	*2165.2288*	1083.1181
439.3027	*220.1550*	537.2796	269.1435	4	L	19	*2096.2074*	1048.6073	---	---
567.3977	284.2025	665.3746	333.1909	5	K	18	1983.1233	992.0653	---	---
696.4403	348.7238	794.4172	397.7122	6	E	17	1855.0284	928.0178	---	---
824.5352	412.7713	922.5121	461.7597	7	K	16	1725.9858	863.4965	---	---
921.5880	461.2976	1019.5649	510.2861	8	P	15	1597.8908	799.4490	---	---
1018.6408	509.8240	1116.6177	558.8125	9	P	14	1500.8380	750.9227	---	---
1105.6728	553.3400	1203.6497	602.3285	10	S	13	1403.7853	702.3963	---	---
1192.7048	596.8561	1290.6817	645.8445	11	S	12	1316.7532	658.8803	---	---
1249.7263	625.3668	1347.7032	674.3552	12	G	11	1229.7212	615.3642	---	---
1377.8213	689.4143	1475.7982	738.4027	13	K	10	1172.6997	586.8535	---	---
1505.8798	753.4436	1603.8567	802.4320	14	Q	9	1044.6048	522.8060	---	---
1592.9119	796.9596	1690.8888	845.9480	15	S	8	916.5462	458.7767	---	---
1705.9959	853.5016	1803.9728	902.4901	16	I	7	829.5142	415.2607	---	---
1819.0800	910.0436	1917.0569	959.0321	17	L	6	716.4301	358.7187	---	---
1906.1120	953.5596	*2004.0889*	1002.5481	18	S	5	603.3461	302.1767	---	---
2005.1804	1003.0939	*2103.1573*	1052.0823	19	V	4	516.3140	258.6606	---	---
2161.2815	1081.1444	*2259.2584*	1130.1329	20	R	3	417.2456	*209.1264*	---	---
2274.3656	1137.6864	*2372.3425*	1186.6749	21	L	2	261.1445	---	---	---
---	---	---	---	22	E	1	*148.0604*	---	---	---

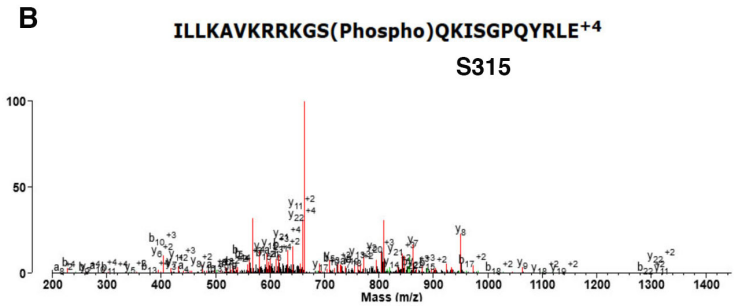

Main Sequence Ions

b-H_3PO_4	b-$H_3PO_4^{+2}$	b	b^{+2}				y	y^{+2}	y-H_3PO_4	y-$H_3PO_4^{+2}$
---	---	---	---	1	I	23	---	---	---	---
---	---	227.1754	---	2	L	22	*2635.4920*	1318.2496	*2537.5151*	1269.2612
---	---	340.2595	---	3	L	21	*2522.4079*	1261.7076	*2424.4310*	1212.7191
---	---	468.3544	234.6809	4	K	20	*2409.3238*	1205.1656	*2311.3469*	1156.1771
---	---	539.3915	270.1994	5	A	19	*2281.2289*	1141.1181	*2183.2520*	1092.1296
---	---	638.4600	319.7336	6	V	18	*2210.1918*	1105.5995	*2112.2149*	1056.6111
---	---	766.5549	383.7811	7	K	17	*2111.1233*	1056.0653	*2013.1465*	1007.0769
---	---	922.6560	461.8317	8	R	16	*1983.0284*	992.0178	*1885.0515*	943.0294
---	---	1078.7571	539.8822	9	R	15	*1826.9273*	913.9673	*1728.9504*	864.9788
---	---	1206.8521	603.9297	10	K	14	*1670.8262*	835.9167	*1572.8493*	786.9283
---	---	1263.8736	632.4404	11	G	13	*1542.7312*	771.8692	1444.7543	722.8808
1332.8950	666.9512	1430.8719	715.9396	12	S(Phospho)	12	*1485.7097*	743.3585	1387.7328	694.3701
1460.9536	730.9804	*1558.9305*	779.9689	13	Q	11	1318.7114	659.8593	---	---
1589.0486	795.0279	*1687.0255*	844.0164	14	K	10	1190.6528	595.8300	---	---
1702.1326	851.5700	*1800.1095*	900.5584	15	I	9	1062.5578	531.7826	---	---
1789.1647	895.0860	*1887.1416*	944.0744	16	S	8	949.4738	475.2405	---	---
1846.1861	923.5967	*1944.1630*	972.5852	17	G	7	862.4417	431.7245	---	---
1943.2389	972.1231	*2041.2158*	1021.1115	18	P	6	805.4203	403.2138	---	---
2071.2975	1036.1524	*2169.2744*	1085.1408	19	Q	5	708.3675	354.6874	---	---
2234.3608	1117.6840	*2332.3377*	1166.6725	20	Y	4	580.3089	290.6581	---	---
2390.4619	1195.7346	*2488.4388*	1244.7230	21	R	3	417.2456	209.1264	---	---
2503.5460	1252.2766	*2601.5229*	1301.2651	22	L	2	261.1445	---	---	---
---	---	---	---	23	E	1	*148.0604*	---	---	---

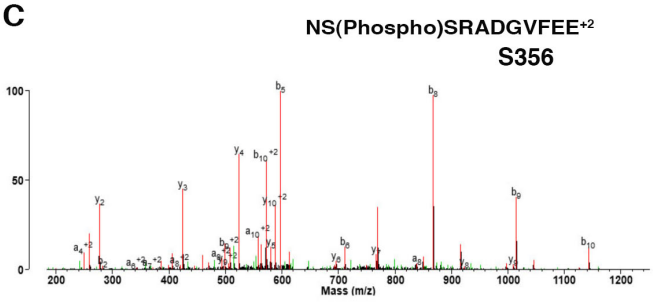

Main Sequence Ions

b-H_3PO_4	b-$H_3PO_4^{+2}$	b	b^{+2}				y	y^{+2}	y-H_3PO_4	y-$H_3PO_4^{+2}$
---	---	---	---	1	N	11	---	---	---	---
184.0717	---	282.0486	---	2	S(Phospho)	10	1176.4569	588.7321	1078.4800	539.7436
271.1037	---	369.0806	---	3	S	9	1009.4585	505.2329	---	---
427.2048	214.1060	525.1817	263.0945	4	R	8	922.4265	461.7169	---	---
498.2419	249.6246	596.2188	298.6130	5	A	7	766.3254	---	---	---
613.2689	307.1381	711.2458	356.1265	6	D	6	695.2883	---	---	---
670.2903	335.6488	768.2672	384.6372	7	G	5	580.2613	---	---	---
769.3587	385.1830	867.3356	434.1715	8	V	4	523.2399	---	---	---
916.4272	458.7172	1014.4041	507.7057	9	F	3	424.1714	---	---	---
1045.4697	523.2385	1143.4466	572.2270	10	E	2	277.1030	---	---	---
---	---	---	---	11	E	1	*148.0604*	---	---	---

Figure S5, related to Figure 5. Annotated LC-MS/MS identifying Ang II-sensitive phosphorylation sites.
A) S128; B) S315; C) S356. Observed *b* and *y* ions are shown in red in the ion spectra plots and tables.

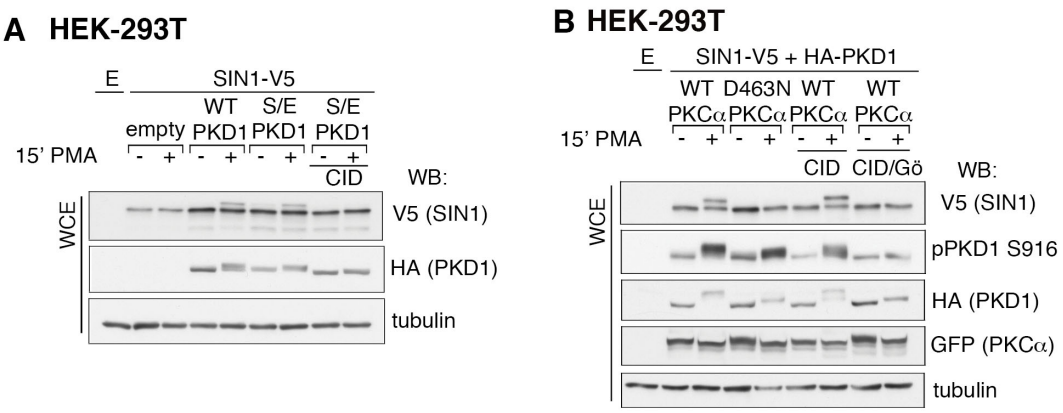

Figure S6, related to Figure 5. PKD activation induces phosphorylation of SIN1.
(A) WB analysis of WCE derived from HEK-293T cells transfected with empty vector, WT PKD1 or constitutively active PKD1 (S738/742E) and WT SIN1-V5. Cells were serum-starved overnight before stimulation with 1 μM PMA either in the presence of vehicle (DMSO) or 25 μM CID655763 (CID).E, empty vector.
(B) WB analysis of WCE derived from HEK-293T cells transfected with WT SIN1-V5 and HA-PKD1 and either WT PKCα or PKCαD463N. Cells were stimulated with PMA in the presence of the indicated inibitors (5 μM Gö6976 (Gö), 25 μM CID655763 (CID)) as described in 'B'. E, empty vector.
(A and B, 2 biological replicates)

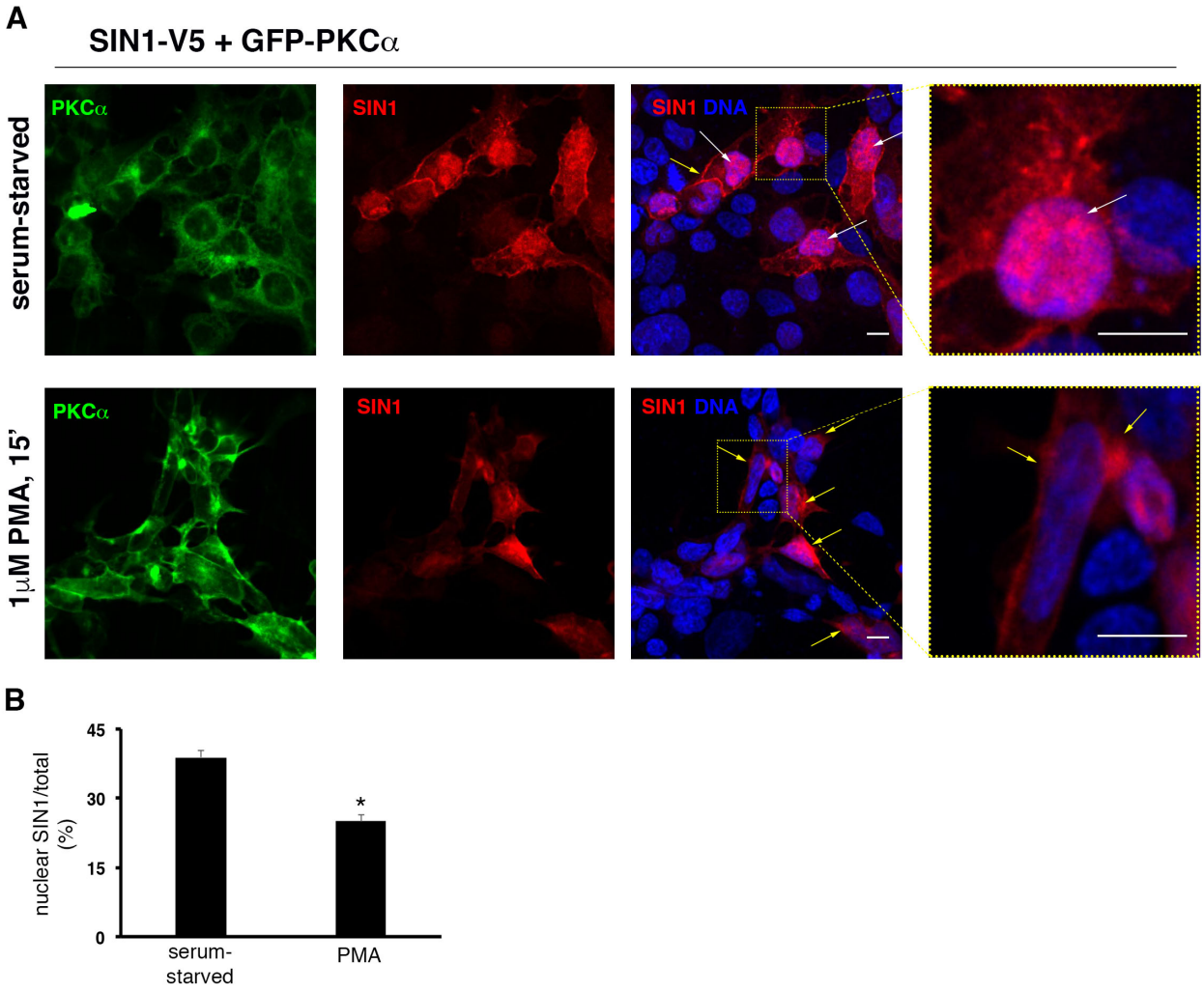

Figure S7, related to Figure 7. PKCα activation relocates SIN1 from the nucleas to a perinuclear compartment and plasma membrane.
(A) SIN1$^{-/-}$ HEK-293T cells expressing WT GFP-PKCα and WT SIN1-V5 were serum-starved overnight and then left unstimulated or stimulated with 1 μM PMA for 15 min. Cells were then processed in a immunofluorescence assay to detect SIN1, costained with DAPI to detect nuclei and imaged by confocal microscopy. White arrows indicate nuclear localized SIN1 and yellow arrows indicate plasma membrane and peri-nuclear localized SIN1. Scale Bar, 10 μM.
(B) Quantification of nuclear SIN1 localization as a percantage of total SIN1. Graph represents mean +/- SEM *$p < 0.001$. (n= 2 biological replicates; serum-starved n=32 cells; PMA-treated, n=53 cells)

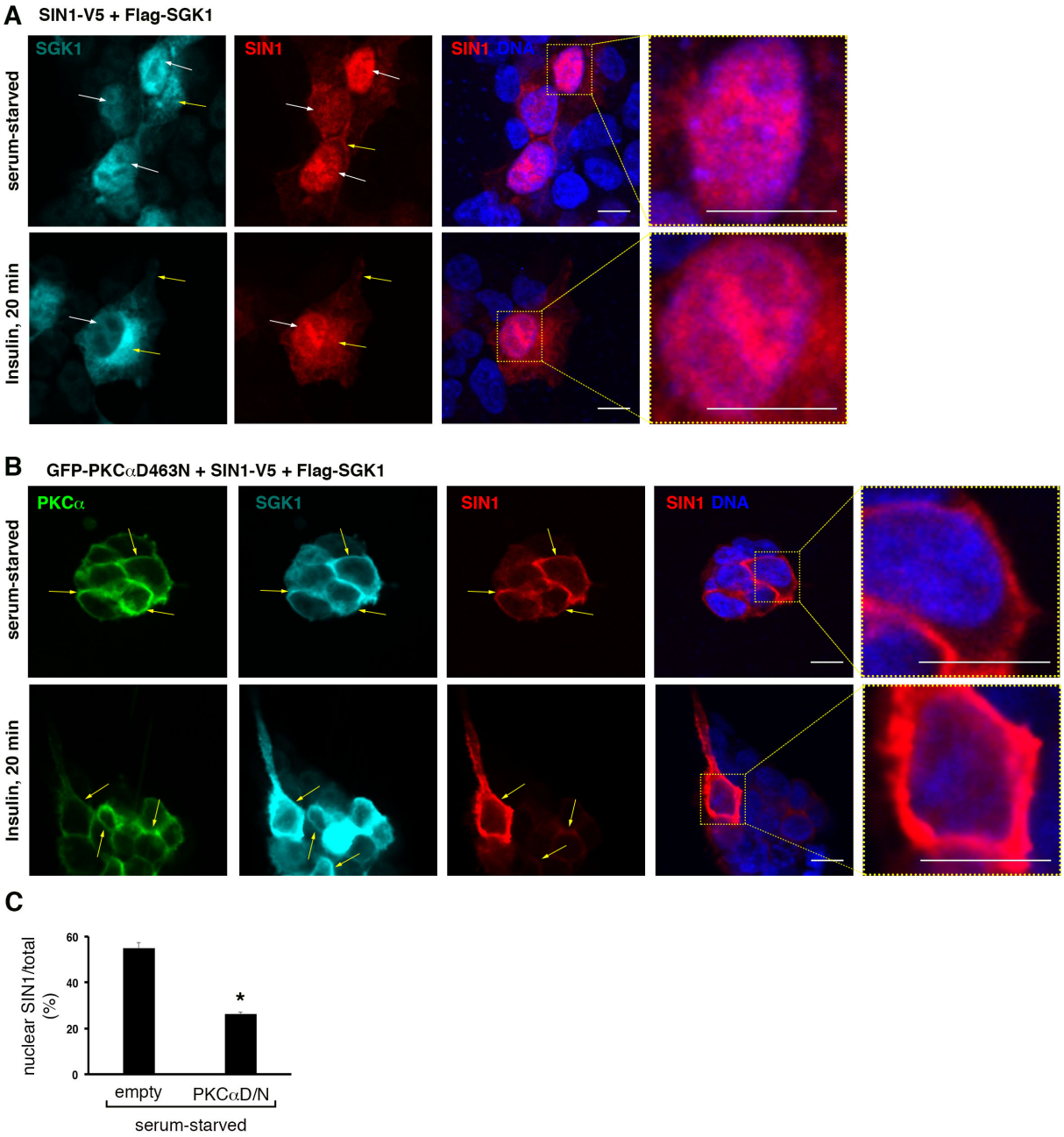

Figure S8, related to Figure 7. PKCαD463N relocates SIN1 and SGK1 from the nucleus and peri-nuclear compartment to the plasma membrane in the absence of hormonal stimulation. SIN1$^{-/-}$ HEK-293T cells expressing WT SIN1-V5, Flag-SGK1 and either empty vector (A) or GFP-PKCαD463N (PKCαD/N) (B) were serum-starved over night and then left unstimulated or stimulated with 200nM insulin for 20 min. Cells were then processed in an immunofluorescence assay to detect SIN1 or SGK1, costained with DAPI to detect nuclei and imaged by confocal microscopy. White arrows indicate nuclear localized SIN1 and SGK1 and yellow arrows indicate plasma membrane and peri-nuclear staining. (n=4 biological replicates for empty vs PKCDN, serum-starved; n=3 biological replicates for empty vs PKCDN, insulin stimulated) (C) Quantification of nuclear localized SIN1 as a percentage of total in serum-starved cells. Graph represents the mean +/- SEM. *$p < 0.0001$ (WT serum-starved, n=38 cells; PKCαD/N serum-starved, n=54 cells).

Table S1. List of phosphopeptides identified in SIN1 by LC-MS/MS (tryptic digestions)

Expectation value	Phosphopeptide	Phosphorylation	*m/z*	Charge
5.30E-05	M(Met-loss+Acetyl)AFLDNPT*IILAHIR	T8	858.4505	2+
6.60E-04	SLFEKKS*LK	S128	580.3101	2+
9.20E-03	EKPPS*SGKQSILSVR	135I136 (ambiguous)	846.9397	2+
6.00E-05	FGFS*TLALVEK	S260	646.3203	2+
1.20E-04	YSS*PGLTSK	S270	510.2264	2+
4.60E-05	YSSPGLTS*KESLFVR	274I275 (ambiguous)	875.9246	2+
3.30E-04	YSSPGLTSKES*LFVR	S278	875.9249	2+
3.10E-05	INAAHGFS*LIQVDNTK	S290	904.4411	2+
1.80E-05	INAAHGFS*LIQVDNTKVTMK	S290	756.3809	3+
1.10E-03	KGS*QKIS*GPQYR	S315	754.8399	2+
5.70E-04	GSQKIS*GPQYR	S319	650.8057	2+
1.10E-03	KGS*QKIS*GPQYR	S315 and S319	754.8399	2+
1.70E-04	ENSS*RADGVFEEDSQIDIATVQDM+LSSHHYK	356I357 (ambiguous)	901.8951	4+
3.00E-03	ENSS*RADGVFEEDSQIDIATVQDMLSSHHYK	356I357 (ambiguous)	897.8961	4+
1.70E-03	ADGVFEEDS*QIDIATVQDMLSSHHYK	S367	1005.7702	3+
2.60E-03	RTS*FSFQK	S510	540.7474	2+

S* or T* denotes phosphorylated serine or threonine. M+ denotes oxidized methionine.

Table S2. List of phosphopeptides identified in SIN1 by LS-MS/MS (GluC digestions)

Expectation value	Phosphopeptide	Phosphorylation	*m/z*	Charge
1.80E-05	KTHPPS*VPGDSGSE	S45	737.8126	2+
1.30E-04	KTHPPSVPGDSGSEVQGS*S*GE	S57;S58	1099.9342	2+
2.30E-04	KKS*LKEKPPSSGKQSILSVRLE	S128	840.4711	3+
1.60E-03	KYSS*PGLTSKE	S270	638.7895	2+
2.60E-03	ILLKAVKRRKGS*QKISGPQYRLE	S315	687.9012	4+
1.10E-03	NS*SRADGVFEE	S356	645.7535	2+

S* or T* denotes phosphorylated serine or threonine.